Bifurcation Analysis of Chemical Reactors with Energy Feedback

Jan Langdeel Pedersen (s082787)

Advisors: Morten Brøns, DTU Compute

Jakob Kjøbsted Huusom, DTU Chemical Engineering

Martin Dan Palis Sørensen, Haldor Topsøe

September 1, 2013

DTU - Technical University of Denmark

Master Thesis

30 ECTS Points

Abstract

This thesis is a study of packed-bed reactors with integrated heat exchangers with focus on bifurcation analysis. A mathematical model of a packed-bed reactor is derived using the molar mass- and energy balance equations. This model is discretized using the method of lines in order to make simulations of the steady state of the system. Furthermore disturbances are added to the inlet conditions and it is shown through simulations that this causes moving hot spots as a consequence of the convective instability of the system. An analysis of the parameters' effect on the steady state is performed together with a bifurcation analysis that shows that no bifurcations occurs in a given parameter space that covers many different processes in the chemical industry.

The theory of a heat exchanger is presented and a model of a such is derived. This model is integrated with the model of the packed-bed reactor in order to perform simulations and bifurcation analysis. Simulations show that disturbances are amplified in the reactor and fed back through the heat exchanger causing growing temperature waves. It turns out that these waves stop growing and end up oscillating with a constant amplitude. This is confirmed by bifurcation analysis that shows the occurrence of both Hopf- and limit point bifurcations. It is shown that bifurcations only occur for changes in the Damköhler number, the dimensionless adiabatic temperature rise, the flow factor and the dimensionless temperature approach. Finally it is shown that a cooled reactor lowers the amount of bifurcations.

Contents

Preface

This master thesis is the product of work done between March 11 and September 1, 2013. It corresponds to 30 ECTS points and has been written at the Technical University of Denmark (DTU) under the guidance of professor Morten Brøns, assistant professor Jakob Kjøbsted Huusom and Martin Dan Palis Sørensen from Haldor Topsøe. I have aimed to make the report as easy to understand as possible, but to fully understand the theory of the report, knowledge of mathematical modelling, finite difference methods and bifurcation analysis will benefit the reader.

My advisors have been excellent at giving me inspiration, guidance and ideas throughout the working period and I am very thankful for their advice. Furthermore, I would like to thank Thomas Pedersen, a fellow student, for reading the report and giving me constructive criticism in the last stage of the project.

Kgs. Lyngby, September 1, 2013

Jan Langdeel Pedersen, s082787

Chapter 1

Introduction

Many important reactions in the chemical industry take place in packed-bed reactors, i.e. tubular reactors filled with catalyst material. These reactors are typically connected to a heat exchanger that is used to heat up the inlet gas with the energy of the outlet gas.
In packed-bed reactors, the convective transport of heat and matter occur at different velocities and cause convective instability that can result in an amplification of process disturbances[1] on the inlet temperature. This causes travelling temperature waves which are not desirable as they, if the temperatures are high enough, might pose a safety hazard if the reactor overheats. It can also be a costly affair if the high temperatures deactivate the catalyst, which then need to be replaced. When the reactor is integrated with a heat exchanger, the amplified disturbances will be fed back to the inlet of the reactor and cause a snowball effect of growing temperatures which make the situation even worse. Therefore a bifurcation analysis will be performed to see which parameter ranges should be avoided to keep the system stable and avoid travelling temperature waves.
The analysis consists of two phases. The first phase of this report only deals with the packed-bed reactor while the second part connects the model of the reactor to a model of a heat exchanger.
To analyse the reactor it is assumed that the gas phase reactions are of the type

$$A \longrightarrow B, \quad \Delta H < 0,$$

[1]The disturbances can be causes by e.g. failure of an electrical pre-heater or failure of a flow valve that suddenly opens or closes.

i.e. standard exothermic reactions. It will furthermore be assumed that there is no radial dispersion, which means that it is sufficient to deal with a one-dimensional model. This model will be derived and turned into dimensionless form in chapter 2. It turns out to have the form

$$\begin{aligned} \frac{\partial y_1}{\partial \tau} &= -Da \exp\left(\gamma\left(1-1/y_2\right)\right) y_1 + \frac{1}{Pe_m}\frac{\partial^2 y_1}{\partial x^2} - \frac{\partial y_1}{\partial x}, \\ Le\frac{\partial y_2}{\partial \tau} &= \beta Da \exp\left(\gamma\left(1-1/y_2\right)\right) y_1 + \frac{1}{Pe_h}\frac{\partial^2 y_2}{\partial x^2} - \frac{\partial y_2}{\partial x} - H_w\left(y_2 - y_{2w}\right) \end{aligned} \tag{1.1}$$

with appropriate initial and boundary conditions. y_1 is the dimensionless concentration and y_2 is the dimensionless temperature while Da, γ, Le, β, Pe_m and Pe_h are different parameters. A literature study is performed to provide a picture of what can be expected when the model is analysed. This analysis takes places in the following chapters. At first the model is implemented in MatLab. This is done using the method of lines discretization. Different simulations are then made to show how the concentration and temperature profiles develop over time and how the system behaves when a process disturbance is added to the inlet conditions.

A lot of different dimensionless parameters are introduced as the model is derived and to provide some insight to these, a study of the parameter effects is made. Here, the parameters are changed independently of each other to see what effect each of the parameters have on the steady state.

The bifurcation analysis of the packed-bed reactor model is done in chapter 6. The different parameters in the model are alternately used as the independent variable to check whether any bifurcations occur when the parameters are changed. The bifurcation analysis is performed using the MatLab-package MatCont.

In the second phase of the report, a model of a heat exchanger is derived and integrated with the packed-bed reactor model. This heat exchanger model is a lot simpler than the model of the reactor as it only consists of algebraic equations. It has the form

$$\begin{aligned} \lambda_1 &= \lambda_3 - \Delta\lambda_{app}, \\ \lambda_2 &= \alpha\lambda_0 + (1-\alpha)\lambda_1, \end{aligned}$$

where λ_0 is the dimensionless inlet temperature to the system, λ_1 is the dimensionless outlet temperature of the heat exchanger, λ_2 is the dimensionless temperature of the inlet gas to the reactor and λ_3 is the dimensionless temperature of the outlet gas of the reactor. Two new parameters, $\Delta\lambda_{app}$ and α are also introduced. $\Delta\lambda_{app}$ is the dimensionless temperature

approach and α is the amount of gas that by-passes the heat exchanger. This parameter is consequently used to control the inlet temperature of the gas to the reactor and will therefore play a crucial role in terms of stability issues.

This is then implemented in MatLab and simulations of the system behaviour are made to see how the complete system reacts to process disturbances. Simulations are also done for different values of α and $\Delta\lambda_{app}$ to see how they affect the concentration and temperature profiles.

Finally, bifurcation analysis is performed on the complete system model. The analysis will focus on the new parameters, α and $\Delta\lambda_{app}$ and the parameters that effected the packed-bed reactor model the most.

Chapter 2

The Packed-Bed Reactor Model

Before any analysis can be done, the model of the concentration and temperature dynamics in a packed-bed reactor needs to be derived. It is assumed that the reactor has the shape of a cylinder and hence, to derive the model equations, a cylinder-shaped control volume is considered, see figure 2.1. The endpoints of this volume lie at z and $z + \Delta z$ and the volume therefore has length Δz. The lateral area is S, which means that the total volume is $\Delta V = \Delta z S$. As this is a packed-bed reactor, the gas volume itself is $\epsilon_B \Delta V$ and the catalyst volume is $(1 - \epsilon_B)\Delta V$. ϵ_B is the bed porosity, defined as

$$\epsilon_B = \frac{V_V}{V_T},$$

where V_V is the void space and V_T is the total volume. This means that this number denotes the fraction of the control volume which is not catalyst material, i.e. void.

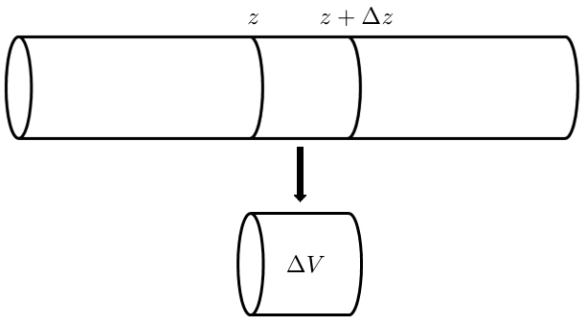

Figure 2.1: The reactor and the control volume.

In the following sections the model equations describing the concentration and temperature

dynamics will be derived. The starting point of this derivation will be the mass- and energy-balance equations.

2.1 The Molar Mass Balance Equation

The general non-stationary molar mass balance equation of the reactant, A, is considered first. This is, according to [2], given by

$$M_{in} + M_{gen} - M_{out} = M_{acc}, \tag{2.1}$$

where M_{in} is the total molar mass of reactant flowing into the control volume, M_{gen} is the total molar mass of reactant generated in the control volume, M_{out} is the total molar mass of reactant flowing out of the control volume and M_{acc} is the total molar mass of reactant that has been accumulated in the control volume from time t to $t + \Delta t$.

What goes into the control volume at z during the time Δt is the concentration of reactant, c, times the time, Δt, times the flow rate. The flow rate is given by $v_z S$, where v_z is the gas velocity. This is however not all. The molar mass can also be transported by movements on the molecular level and M_{in} will therefore also include a dispersion term. This means that

$$M_{in} = -D\frac{\partial c}{\partial z}\bigg|_z S\Delta t + c\big|_z v_z S\Delta t. \tag{2.2}$$

The first term is due to dispersion and is given by Fick's law, see [14]. Here D plays the role of the dispersion coefficient.

The general reaction that occurs in the packed-bed reactor is first-order exothermic and can be written as

$$A \longrightarrow B, \quad \Delta H < 0,$$

where A is the reactant, B is the product of the reaction and ΔH is the change in enthalpy. Enthalpy is a measure of the total energy in the system. The reaction rate of A is

$$R_A = k_0 e^{-E_a/RT} c^n,$$

where k_0 is a rate constant, E_a is the activation energy, R is the gas constant, T is the temperature and n is the order of the reaction. As this is assumed to be a first-order reaction,

$n = 1$ and the reaction rate can therefore be written as

$$R_A = k_0 e^{-E_a/RT} c.$$

The rate of disappearance is then, by convention, given as

$$-R_A = -k_0 e^{-E_a/RT} c.$$

The reaction only proceeds on the surface of the catalyst. The catalyst itself has a micro pore structure meaning that the surface of the catalyst is very large. This means that the catalyst volume is a good measure for the volume in which the reaction proceeds. Assuming that the control volume has been chosen so small that the concentration is spatially uniform throughout the control volume, the mass generated can then, according to [1], be written as

$$\begin{aligned} M_{gen} &= -R_A(1-\epsilon_B)\Delta V \Delta t \\ &= -k_0 e^{-E_a/RT} c(1-\epsilon_B) S \Delta z \Delta t. \end{aligned} \tag{2.3}$$

Using the same arguments as for M_{in}, the total mass that exits the control volume can be written as

$$M_{out} = -D\frac{\partial c}{\partial z}\bigg|_{z+\Delta z} S\Delta t + c|_{z+\Delta z} v_z S \Delta t. \tag{2.4}$$

Finally, the accumulated mass will be discussed. This is the mass of A in the control volume at time $t + \Delta t$ minus the mass of A at time t. This means that

$$\begin{aligned} M_{acc} &= m_A|_{t+\Delta t} - m_A|_t \\ &= \epsilon_B \Delta V \left(c|_{t+\Delta t} - c|_t\right) \\ &= \epsilon_B S \Delta z \left(c|_{t+\Delta t} - c|_t\right) \end{aligned} \tag{2.5}$$

as $c = m_A/\epsilon_B \Delta V$.

Inserting (2.2)-(2.5) into (2.1) yields

$$\begin{aligned} &\epsilon_B S \Delta z \left(c|_{t+\Delta t} - c|_t\right) \\ &= -D\frac{\partial c}{\partial z}\bigg|_z S\Delta t + c\big|_z v_z S\Delta t - k_0 e^{-E_a/RT} c(1-\epsilon_B) S\Delta z \Delta t + D\frac{\partial c}{\partial z}\bigg|_{z+\Delta z} S\Delta t - c|_{z+\Delta z} v_z S \Delta t. \end{aligned}$$

Rearranging and collecting terms yields

$$\begin{aligned}
\epsilon_B S\Delta z\left(c|_{t+\Delta t}-c|_t\right) &= DS\Delta t\left(\left.\frac{\partial c}{\partial z}\right|_{z+\Delta z}-\left.\frac{\partial c}{\partial z}\right|_z\right)\\
&\quad - v_z S\Delta t\left(c|_{z+\Delta z}-c|_z\right)-k_0 e^{-E_a/RT}c(1-\epsilon_B)S\Delta z\Delta t \quad \Leftrightarrow\\
\epsilon_B\left(c|_{t+\Delta t}-c|_t\right) &= \frac{D}{\Delta z}\Delta t\left(\left.\frac{\partial c}{\partial z}\right|_{z+\Delta z}-\left.\frac{\partial c}{\partial z}\right|_z\right)\\
&\quad - \frac{v_z}{\Delta z}\Delta t\left(c|_{z+\Delta z}-c|_z\right)-k_0 e^{-E_a/RT}c(1-\epsilon_B)\Delta t \quad \Leftrightarrow\\
\epsilon_B\frac{c|_{t+\Delta t}-c|_t}{\Delta t} &= D\left(\frac{\left.\frac{\partial c}{\partial z}\right|_{z+\Delta z}-\left.\frac{\partial c}{\partial z}\right|_z}{\Delta z}\right)-v_z\left(\frac{c|_{z+\Delta z}-c|_z}{\Delta z}\right)-k_0(1-\epsilon_B)e^{-E_a/RT}c.
\end{aligned}$$

By letting $\Delta z\to 0$, $\Delta t\to 0$ and then using the definition of the derivative, one obtains

$$\epsilon_B\frac{\partial c}{\partial t}=D\frac{\partial^2 c}{\partial z^2}-v_z\frac{\partial c}{\partial z}-(1-\epsilon_B)k_0 ce^{-E_a/RT}, \tag{2.6}$$

which is the packed-bed reactor model equation for the concentration dynamics.

2.2 The Energy Balance Equation

Next, the equation for the temperature dynamics will be derived. This will be based on the non-stationary energy balance equation that, according to [2], is analogous to the mass balance from before. This means that

$$E_{in}+E_{gen}-E_{out}=E_{acc}, \tag{2.7}$$

where E_{in} is the amount of energy entering the control volume, E_{gen} is the energy generated in the control volume, E_{out} is the energy leaving the control volume and E_{acc} is the energy accumulated in the control volume from time t to $t+\Delta t$.

For the heat flow into the control volume there are two things to take into account. First, the heat related to mass flow and second, the heat related to thermal movements. The mass that enters because of the flow is $m=v_z S\rho_g\Delta t$, where ρ_g is the density of the gas. Using the relationship between mass and heat, the total energy that enters because of the flow is

$$\begin{aligned}
Q_1 &= C_{pg}mT|_z\\
&= C_{pg}v_z S\rho_g\Delta tT|_z,
\end{aligned}$$

where C_{pg} is the heat capacity of the gas and T is the temperature.
The energy that passes a plane, z, per time- and area-unit is, according to [14], defined by Fourier's law of heat conduction as

$$q_y = -k\frac{\partial T}{\partial z}\bigg|_z,$$

where k is the coefficient of thermal conductivity. This means that the heat entering the control volume during the time Δt will be

$$Q_2 = -k\frac{\partial T}{\partial z}\bigg|_z S\Delta t.$$

Hence, the total amount of energy entering is

$$\begin{aligned} E_{in} &= Q_1 + Q_2 \\ &= C_{pg}v_z S\rho_g \Delta t T|_z - k\frac{\partial T}{\partial z}\bigg|_z S\Delta t. \end{aligned} \tag{2.8}$$

The energy generated is related to the generated mass by the change in enthalpy. As the system is exothermic the change in enthalpy is $-\Delta H$, which means that the total energy generated is

$$E_{gen} = (-\Delta H)\,(1-\epsilon_B)\,ck_0 e^{-Ea/RT} S\Delta z\Delta t. \tag{2.9}$$

Even though there is no concentration dispersion in the radial direction there is still some heat transfer between the reaction mixture and the reactor wall. The rate of this heat transfer can be written as

$$q_w = U_w A_w\,(T - T_w)\,,$$

where U_w is the overall heat transfer coefficient. This is the reciprocal of the sum of the resistances to the heat transfer in the form of a film that covers the reactor wall and, eventually, dirt. A_w is the heat transfer surface area of the wall and T_w is the temperature of the wall. The bed is in the shape of a cylinder so the surface area of the control volume is

$$A_w = \pi d_B \Delta z,$$

where d_B is the diameter of the bed. This means that

$$q_w = U_w \pi d_B \Delta z\,(T - T_w)\,.$$

By using the same arguments as for E_{in} the total energy leaving the control volume is

$$E_{out} = C_{pf} v_z S \rho_g \Delta t T|_{z+\Delta z} - k \frac{\partial T}{\partial z}\bigg|_{z+\Delta z} S\Delta t + U_w \pi d_B \Delta z \left(T - T_w\right) \Delta t. \tag{2.10}$$

The energy accumulated is

$$\begin{aligned} E_{acc} &= Q|_{t+\Delta t} - Q|_t \\ &= C_p m \left(T|_{t+\Delta t} - T|_t\right) \\ &= C_p \rho S \Delta z \left(T|_{t+\Delta t} - T|_t\right), \end{aligned}$$

where C_p, m, and ρ are the heat capacity, mass and density of all the substance in the control volume respectively. By using the bed porosity to distinguish between the gas and the solid catalyst this can be written as

$$E_{acc} = S\Delta z \left(\epsilon_B \rho_g C_{pg} + \left(1 - \epsilon_B\right) \rho_s C_{ps}\right) \left(T|_{t+\Delta t} - T|_t\right), \tag{2.11}$$

where ρ is density, C_p is heat capacity and the subscripts g and s denotes gas and solid catalyst respectively.

Inserting (2.8)-(2.11) into (2.7) yields

$$\begin{aligned} &S\Delta z \left(\epsilon_B \rho_g C_{pg} + \left(1 - \epsilon_B\right) \rho_s C_{ps}\right) \left(T|_{t+\Delta t} - T|_t\right) = C_{pf} v_z S \rho_g \Delta t T|_z - k \frac{\partial T}{\partial z}\bigg|_z S\Delta t \\ &+ \left(-\Delta H\right) \left(1 - \epsilon_B\right) c k_0 e^{-E_a/RT} S\Delta z \Delta t - C_{pf} v_z S \rho_g \Delta t T|_{z+\Delta z} \\ &+ k \frac{\partial T}{\partial z}\bigg|_{z+\Delta z} S\Delta t - U_w \pi d_B \Delta z \left(T - T_w\right) \Delta t. \end{aligned}$$

Collecting terms and dividing by $S\Delta z$ on both sides makes the equation

$$\begin{aligned} &\left(\epsilon_B \rho_g C_{pg} + \left(1 - \epsilon_B\right) \rho_s C_{ps}\right) \left(T|_{t+\Delta t} - T|_t\right) = \frac{k\Delta t}{\Delta z} \left(\frac{\partial T}{\partial z}\bigg|_{z+\Delta z} - \frac{\partial T}{\partial z}\bigg|_z\right) \\ &- \frac{C_{pg} v_z \rho_g \Delta t}{\Delta z} \left(T|_{z+\Delta z} - T|_z\right) + \left(-\Delta H\right) \left(1 - \epsilon_B\right) c k_0 e^{-Ea/RT} \Delta t - \frac{U_w \pi d_B \Delta t}{S} \left(T - T_w\right) \quad \Leftrightarrow \\ &\left(\epsilon_B \rho_g C_{pg} + \left(1 - \epsilon_B\right) \rho_s C_{ps}\right) \frac{T|_{t+\Delta t} - T|_t}{\Delta t} = k \frac{\frac{\partial T}{\partial z}\Big|_{z+\Delta z} - \frac{\partial T}{\partial z}\Big|_z}{\Delta z} \\ &- C_{pg} \rho_g v_z \frac{T|_{z+\Delta z} - T|_z}{\Delta z} + \left(-\Delta H\right) \left(1 - \epsilon_B\right) c k_0 e^{-Ea/RT} - \frac{U_w \pi d_B}{S} \left(T - T_w\right). \end{aligned}$$

By letting $\Delta z \to 0$, $\Delta t \to 0$ and using the definition of the derivative and the fact that

$S = \pi d_B^2/4$ this becomes

$$\begin{aligned}(\epsilon_B \rho_g C_{pg} + (1-\epsilon_B)\,\rho_s C_{ps})\,\frac{\partial T}{\partial t} &= k\frac{\partial^2 T}{\partial z^2} - C_{pg}\rho_g v_z \frac{\partial T}{\partial t} \\ + (-\Delta H)\,(1-\epsilon_B)\,c k_0 e^{-Ea/RT} &- U_w \frac{4}{d_B}\,(T - T_w)\,,\end{aligned} \tag{2.12}$$

which is the model equation for the temperature of the reaction mixture.

2.3 Initial and Boundary Conditions

The final step in completing the model is to determine the initial- and boundary conditions.

2.3.1 Initial Conditions

The initial concentration of the reactant is 0 as there is no reactant in the bed at time zero. The initial temperature is T_0. This means that the initial conditions are

$$c(z,0) = 0 \quad \wedge \quad T(z,0) = T_0. \tag{2.13}$$

2.3.2 Boundary Conditions

To the immediate left of the inlet boundary, where the gas enters the reactor, there is plug flow, i.e. no dispersion. To the immediate right of this boundary there is dispersion, see figure 2.2.

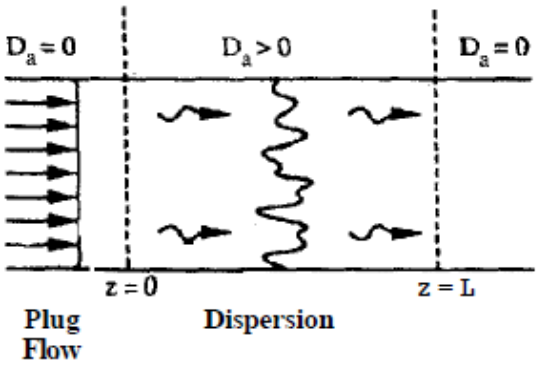

Figure 2.2: Cross section of the reactor model. The figure is found in [1] and D_a plays the role of the dispersion coefficient.

This means that the flow of mass at the immediate left of the inlet boundary is

$$F_m\left(0^-,t\right)=v_zSc\left(0^-,t\right)$$

and at the immediate right of the inlet boundary, the flow of mass is

$$F_m\left(0^+,t\right)=-DS\frac{\partial c}{\partial z}\bigg|_{z=0^+}+v_zSc\left(0^+,t\right).$$

Putting these expressions equal to each other yields

$$\begin{aligned}&v_zSC_A\left(0^-,t\right)=-DS\frac{\partial c}{\partial z}\bigg|_{z=0^+}+v_zSc\left(0^+,t\right)\quad\Leftrightarrow\\&D\frac{\partial c}{\partial z}\bigg|_{z=0^+}+v_z\left(c\left(0^-,t\right)-c\left(0^+,t\right)\right)=0.\end{aligned}\tag{2.14}$$

The flow of heat to the immediate left of the inlet boundary is

$$F_h\left(0^-,t\right)=v_zSC_{pg}\rho_gT\left(0^-,t\right),$$

while it, at the immediate right of the inlet boundary, is

$$F_h\left(0^+,t\right)=-kS\frac{\partial T}{\partial z}\bigg|_{z=0^+}+v_zSC_{pg}\rho_gT\left(0^+,t\right).$$

These expressions are put equal to each other and yield

$$\begin{aligned}&v_zSC_{pg}\rho_gT\left(0^-,t\right)=-kS\frac{\partial T}{\partial z}\bigg|_{z=0^+}+v_zSC_{pg}\rho_gT\left(0^+,t\right)\quad\Leftrightarrow\\&k\frac{\partial T}{\partial z}\bigg|_{z=0^+}+v_zC_{pg}\rho_g\left(T\left(0^-,t\right)-T\left(0^+,t\right)\right)=0.\end{aligned}\tag{2.15}$$

It is assumed that no reaction occurs at the second boundary. This means that the concentration and the temperature do not change, i.e. that they have no gradient. Therefore the boundary conditions at the second boundary are

$$\frac{\partial c}{\partial z}\bigg|_{z=L}=0\quad\wedge\quad\frac{\partial T}{\partial z}\bigg|_{z=L}=0.\tag{2.16}$$

The boundary conditions (2.14)-(2.16) are known as the Danckwerts boundary conditions, see [10] and [13].

The complete reactor model is then (2.6) and (2.12) with the initial conditions (2.13) and the boundary conditions (2.14)-(2.16). This model will in the following section be made dimensionless.

2.4 Dimensionless Variables

In order to make the equations dimensionless, some dimensionless variables need to be defined. The dimensionless concentration of reactant is defined as

$$y_1 = \frac{c}{c_0},$$

the dimensionless temperature is defined as

$$y_2 = \frac{T}{T_0},$$

the dimensionless length is defined as

$$x = \frac{z}{L}$$

and the dimensionless time is defined as

$$\tau = \frac{tv_z}{\epsilon_B L}.$$

First, equation (2.6) will be addressed. From the definition of y_1 it follows that

$$\frac{\partial c}{\partial z} = \frac{\partial (c_0 y_1)}{\partial z} = c_0 \frac{\partial y_1}{\partial z}.$$

By using the chain rule, this can be written as

$$\frac{\partial c}{\partial z} = c_0 \frac{\partial y_1}{\partial x}\frac{\partial x}{\partial z},$$

which reduces to

$$\frac{\partial c}{\partial z} = \frac{c_0}{L}\frac{\partial y_1}{\partial x} \tag{2.17}$$

because of the definition of x. In the same way it can be found that

$$\frac{\partial^2 c}{\partial z^2} = \frac{c_0}{L^2}\frac{\partial^2 y_1}{\partial x^2} \tag{2.18}$$

and

$$\frac{\partial c}{\partial t} = \frac{c_0 v_z}{\epsilon_B L}\frac{\partial y_1}{\partial \tau}. \tag{2.19}$$

Inserting the definition of the dependent variables together with (2.17)-(2.19) into (2.6) yields

$$\begin{aligned} \frac{c_0 v_z}{L}\frac{\partial y_1}{\partial \tau} &= \frac{D c_0}{L^2}\frac{\partial^2 y_1}{\partial x^2} - \frac{v_z c_0}{L}\frac{\partial y_1}{\partial x} - (1-\epsilon_B) c_0 y_1 k_0 e^{-E_a/RT_0 y_2} \quad \Leftrightarrow \\ \frac{\partial y_1}{\partial \tau} &= \frac{D}{v_z L}\frac{\partial^2 y_1}{\partial x^2} - \frac{\partial y_1}{\partial x} - \frac{(1-\epsilon_B) L k_0}{v_z} y_1 e^{-E_a/RT_0 y_2}. \end{aligned}$$

The dimensionless activation energy is now defined as

$$\gamma = \frac{E_a}{RT_0}$$

and the Peclet number for mass is, according to [1], defined as

$$Pe_m = \frac{v_z L}{D}.$$

This is, by definition, the ratio of the rate of transport by convection to the rate of transport by dispersion. Inserting these definitions into the model equation yields

$$\begin{aligned}\frac{\partial y_1}{\partial \tau} &= \frac{1}{Pe_m}\frac{\partial^2 y_1}{\partial x^2} - \frac{\partial y_1}{\partial x} - \frac{(1-\epsilon_B)Lk_0}{v_z} y_1 e^{-\gamma/y_2} \quad \Leftrightarrow \\ \frac{\partial y_1}{\partial \tau} &= \frac{1}{Pe_m}\frac{\partial^2 y_1}{\partial x^2} - \frac{\partial y_1}{\partial x} - \frac{(1-\epsilon_B)Lk_0}{v_z} e^{-\gamma} y_1 e^{\gamma(1-1/y_2)}.\end{aligned}$$

The Damköhler number is defined as the reaction rate to the rate of transport by convection at the entrance of the reactor, i.e.

$$Da = \frac{(1-\epsilon_B)Lk_0}{v_z} e^{-\gamma}.$$

Inserting this in the above makes the packed-bed reactor model equation for the concentration dynamics in dimensionless form

$$\frac{\partial y_1}{\partial \tau} = \frac{1}{Pe_m}\frac{\partial^2 y_1}{\partial x^2} - \frac{\partial y_1}{\partial x} - Da\, y_1 e^{\gamma(1-1/y_2)}. \tag{2.20}$$

The equation (2.12) will now be addressed. Just as before it can be shown that

$$\frac{\partial T}{\partial z} = \frac{T_0}{L}\frac{\partial y_2}{\partial x}, \qquad \frac{\partial^2 T}{\partial z^2} = \frac{T_0}{L^2}\frac{\partial^2 y_2}{\partial x^2}, \qquad \frac{\partial T}{\partial t} = \frac{T_0 v_z}{\epsilon_B L}\frac{\partial y_2}{\partial \tau}$$

because of the definition of τ and T. Inserting this in (2.12) yields

$$\begin{aligned}&\left(\epsilon_B \rho_g C_{pg} + (1-\epsilon_B)\,\rho_s C_{ps}\right)\frac{T_0 v_z}{\epsilon_B L}\frac{\partial y_2}{\partial \tau} = k\frac{T_0}{L^2}\frac{\partial^2 y_2}{\partial x^2} - C_{pg}\rho_g v_z \frac{T_0}{L}\frac{\partial y_2}{\partial x} \\ &+ (-\Delta H)\,(1-\epsilon_B)\,ck_0 e^{-E_a/RT} - U_w \frac{4}{d_B}\,(T - T_w)\,.\end{aligned}$$

By defining the dimensionless wall temperature as

$$y_{2w} = \frac{T_w}{T_0}$$

this equation can be rewritten as

$$\begin{aligned}
&\frac{\left(\epsilon_B \rho_g C_{pg} + (1-\epsilon_B)\,\rho_s C_{ps}\right)}{\epsilon_B \rho_g C_{pg}} \frac{T_0 v_z}{L} \frac{\partial y_2}{\partial \tau} = \frac{k T_0}{L^2 \rho_g C_{pg}} \frac{\partial^2 y_2}{\partial x^2} - \frac{v_z T_0}{L} \frac{\partial y_2}{\partial x} \\
&+ \frac{(-\Delta H)\,(1-\epsilon_B)\,c_0 y_1 k_0}{\rho_g C_{pg}} e^{-E_a/RT_0 y_2} - U_w \frac{4}{d_B \rho_g C_{pg}} \left(y_2 T_0 - y_{2w} T_0\right) \quad \Leftrightarrow \\
&\frac{\left(\epsilon_B \rho_g C_{pg} + (1-\epsilon_B)\,\rho_s C_{ps}\right)}{\epsilon_B \rho_g C_{pg}} \frac{\partial y_2}{\partial \tau} = \frac{k}{L \rho_g C_{pg} v_z} \frac{\partial^2 y_2}{\partial x^2} - \frac{\partial y_2}{\partial x} \\
&+ \frac{(-\Delta H)\,(1-\epsilon_B)\,c_0 y_1 k_0 L}{\rho_g C_{pg} T_0 v_z} e^{-E_a/RT_0 y_2} - U_w \frac{4L}{d_B \rho_g C_{pg} v_z} \left(y_2 - y_{2w}\right). \qquad (2.21)
\end{aligned}$$

Just as for mass there is a Peclet number for heat defined by

$$Pe_h = \frac{L v_z \rho_g C_{pg}}{k},$$

which is the ratio of the rate of transport of heat by convection to the rate of transport of heat by dispersion. The Lewis number, Le, is defined as the ratio of the thermal transport time constant to the material transport time constant. This means that

$$Le = \frac{\left(\epsilon_B \rho_g C_{pg} + (1-\epsilon_B)\,\rho_s C_{ps}\right)}{\epsilon_B \rho_g C_{pg}}. \qquad (2.22)$$

Inserting these numbers in equation (2.21) together with the definition of the dimensionless activation energy yields

$$\begin{aligned}
&Le \frac{\partial y_2}{\partial \tau} = \frac{1}{Pe_h} \frac{\partial^2 y_2}{\partial x^2} - \frac{\partial y_2}{\partial x} + \frac{(-\Delta H)\,(1-\epsilon_B)\,c_0 y_1 k_0 L}{\rho_g C_{pg} T_0 v_z} e^{-\gamma/y_2} - \frac{4 L U_w}{d_B \rho_g C_{pg} v_z} \left(y_2 - y_{2w}\right) \quad \Leftrightarrow \\
&Le \frac{\partial y_2}{\partial \tau} = \frac{1}{Pe_h} \frac{\partial^2 y_2}{\partial x^2} - \frac{\partial y_2}{\partial x} + Da y_1 \frac{(-\Delta H)\,c_0}{\rho_g C_{pg} T_0} e^{\gamma(1-1/y_2)} - \frac{4 L U_w}{d_B \rho_g C_{pg} v_z} \left(y_2 - y_{2w}\right).
\end{aligned}$$

By defining the dimensionless adiabatic temperature rise as

$$\beta = \frac{(-\Delta H) c_0}{\rho_g C_{pg} T_0}$$

and the dimensionless overall heat transfer coefficient as

$$H_w = \frac{4 L U_w}{d_B \rho_g C_{pg} v_z}$$

the equation can be written as

$$Le \frac{\partial y_2}{\partial \tau} = \frac{1}{Pe_h} \frac{\partial^2 y_2}{\partial x^2} - \frac{\partial y_2}{\partial x} + \beta Da y_1 e^{\gamma(1-1/y_2)} - H_w \left(y_2 - y_{2w}\right).$$

This is the packed-bed reactor model equation for the temperature dynamics in dimensionless form.

2.4.1 Dimensionless Initial Conditions

Inserting the definition of the dimensionless concentration into the initial condition for the concentration yields

$$\begin{aligned} c_0 y_1(x,0) &= 0 \quad \Leftrightarrow \\ y_1(x,0) &= 0. \end{aligned} \tag{2.23}$$

In the same way it can be found that

$$\begin{aligned} T_0 y_2(x,0) &= T_0 \quad \Leftrightarrow \\ y_2(x,0) &= 1. \end{aligned} \tag{2.24}$$

2.4.2 Dimensionless Boundary Conditions

To derive the dimensionless boundary condition for the concentration at the inlet boundary, (2.17) is inserted in (2.14). This makes the condition

$$\begin{aligned} D\frac{c_0}{L}\frac{\partial y_1}{\partial x}\bigg|_{z=0^+} + v_z\left(c\left(0^-,t\right) - c\left(0^+,t\right)\right) = 0 \quad \Leftrightarrow \\ \frac{\partial y_1}{\partial x}\bigg|_{z=0^+} + \frac{v_z L}{D}\left(y_1\left(0^-,t\right) - y_1\left(0^+,t\right)\right) = 0. \end{aligned}$$

Inserting $Pe_m = v_z L/D$ makes the boundary condition

$$\frac{\partial y_1}{\partial x}\bigg|_{z=0^+} + Pe_m\left(y_1\left(0^-,t\right) - y_1\left(0^+,t\right)\right) = 0.$$

In the same way, (2.15) can be rewritten as

$$\begin{aligned} k\frac{T_0}{L}\frac{\partial y_2}{\partial x}\bigg|_{z=0^+} + v_z C_{pg}\rho_g\left(T\left(0^-,t\right) - T\left(0^+,t\right)\right) = 0 \quad \Leftrightarrow \\ \frac{\partial y_2}{\partial x}\bigg|_{z=0^+} + \frac{v_z C_{pg}\rho_g L}{k}\left(y_2\left(0^-,t\right) - y_2\left(0^+,t\right)\right) = 0 \quad \Leftrightarrow \\ \frac{\partial y_2}{\partial x}\bigg|_{z=0^+} + Pe_h\left(y_2\left(0^-,t\right) - y_2\left(0^+,t\right)\right) = 0. \end{aligned}$$

Finally the boundary conditions for the second boundary will be addressed. The condition for the concentration is

$$\begin{aligned} \frac{\partial c}{\partial z}\bigg|_{z=L} &= 0 \quad \Leftrightarrow \\ \frac{c_0}{L}\frac{\partial y_1}{\partial x}\bigg|_{x=1} &= 0 \quad \Leftrightarrow \\ \frac{\partial y_1}{\partial x}\bigg|_{x=1} &= 0, \end{aligned}$$

while the condition for the temperature is

$$\begin{aligned} \left.\frac{\partial T}{\partial z}\right|_{z=L} &= 0 \quad \Leftrightarrow \\ \left.\frac{T_0}{L}\frac{\partial y_2}{\partial x}\right|_{x=1} &= 0 \quad \Leftrightarrow \\ \left.\frac{\partial y_2}{\partial x}\right|_{x=1} &= 0. \end{aligned}$$

2.5 The Model Equations

To sum up, the dimensionless equations describing the concentration- and temperature dynamics in a packed-bed reactor are

$$\frac{\partial y_1}{\partial \tau} = -Da \exp\left(\gamma\left(1 - 1/y_2\right)\right) y_1 + \frac{1}{Pe_m}\frac{\partial^2 y_1}{\partial x^2} - \frac{\partial y_1}{\partial x}, \tag{2.25}$$

$$Le\frac{\partial y_2}{\partial \tau} = \beta Da \exp\left(\gamma\left(1 - 1/y_2\right)\right) y_1 + \frac{1}{Pe_h}\frac{\partial^2 y_2}{\partial x^2} - \frac{\partial y_2}{\partial x} - H_w\left(y_2 - y_{2w}\right) \tag{2.26}$$

with the initial conditions

$$y_1\left(x, 0\right) = 0 \quad \wedge \quad y_2\left(x, 0\right) = 1. \tag{2.27}$$

The boundary conditions at the inlet boundary are

$$\left.\frac{\partial y_1}{\partial x}\right|_{x=0} + Pe_m\left(y_1\left(0^-, t\right) - y_1\left(0^+, t\right)\right) = 0, \tag{2.28}$$

$$\left.\frac{\partial y_2}{\partial x}\right|_{x=0} + Pe_h\left(y_2\left(0^-, t\right) - y_2\left(0^+, t\right)\right) = 0, \tag{2.29}$$

while the boundary conditions at the outlet boundary are

$$\left.\frac{\partial y_1}{\partial x}\right|_{x=1} = 0, \tag{2.30}$$

$$\left.\frac{\partial y_2}{\partial x}\right|_{x=1} = 0. \tag{2.31}$$

Chapter 3

Literature Study

To obtain an overview of what research has already been done on the subject, a literature study is performed, starting with an examination of what kind of instabilities one can expect when dealing with packed-bed reactors.
According to [4] and [7], an activator is a variable with a tendency to grow, while an inhibitor is a variable that counteracts this tendency. The activator could for example be the heat released in an exothermic reaction, while the inhibitor could be the depletion of reactant in an exothermic reaction. When both these variables are present in a system, this system is called an activator-inhibitor system. If the inhibitor variable balances local fluctuations of the activator, the steady state of the system will remain stable, see figure 3.1a.
On the other hand, if the activator and inhibitor move at different speeds, these waves become phase-shifted, see figure 3.1b. This means that the activator is no longer limited by the inhibitor and will start to grow. This is known as differential-flow instability as it is caused by differential flows. This phenomenon has been verified experimentally in [6].
A packed-bed reactor indeed is an activator-inhibitor system and the activator is heat released in an exothermic reaction. If this activator starts to grow it causes travelling waves of temperature that move through the reactor. These travelling temperature waves have different names in the literature but will, like in [8], be referred to as moving hot spots in this report.

According to [4], the character of differential-flow instability can be either absolute or convective. If a small perturbation makes the system leave its steady state and create a new steady state or dynamic mode, the initial steady state is said to be absolutely unstable.

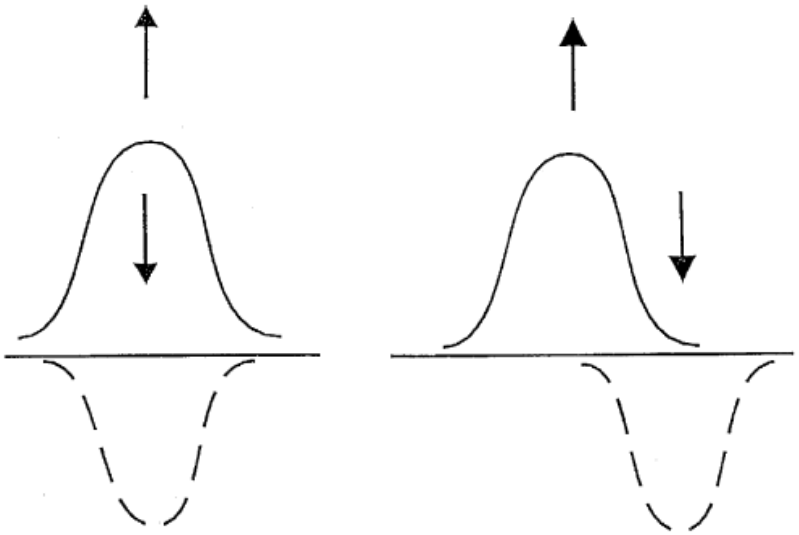

(a) Differential flow is off. (b) Differential flow is on.

Figure 3.1: Stability properties of the steady state of an activator-inhibitor system. The figures are from [4].

On the other hand, if the perturbation is amplified and carried downstream before it is eventually washed out, the system is said to be convectively unstable.

The standard reaction in a packed-bed reactor can be described by equation (1.1). The right hand side of the second equation is scaled by the inverse of the Lewis number, Le^{-1}. This also includes the term with the first spatial derivative, which means that the velocity of heat flow is Le^{-1}, while the velocity of matter flow is 1. According to [8], $Le > 1$ for packed-bed reactors and the velocity of matter flow is therefore greater than the velocity of heat flow. It is these differences in velocities, caused by Le, that are the reasons for differential-flow instability, and hence moving hot spots. Physically it is the reactor packing that acts as a thermal reservoir and slows down the transport of heat compared to that of matter, according to [7].

One can show that this instability actually exists by solving the system numerically. This was done in [4] and [8] with the Danckwerts boundary conditions, which were originally presented in [10]. The calculated steady state for both concentration and temperature can be seen as

the thick lines in figure 3.2 for the parameter values

$$Pe_m = 3000,\ Pe_h = 1000,\ Le = 3,\ \beta = 0.5,\ Da = 0.135,\ \gamma = 22.$$

These steady states will be reproduced in chapter 4.

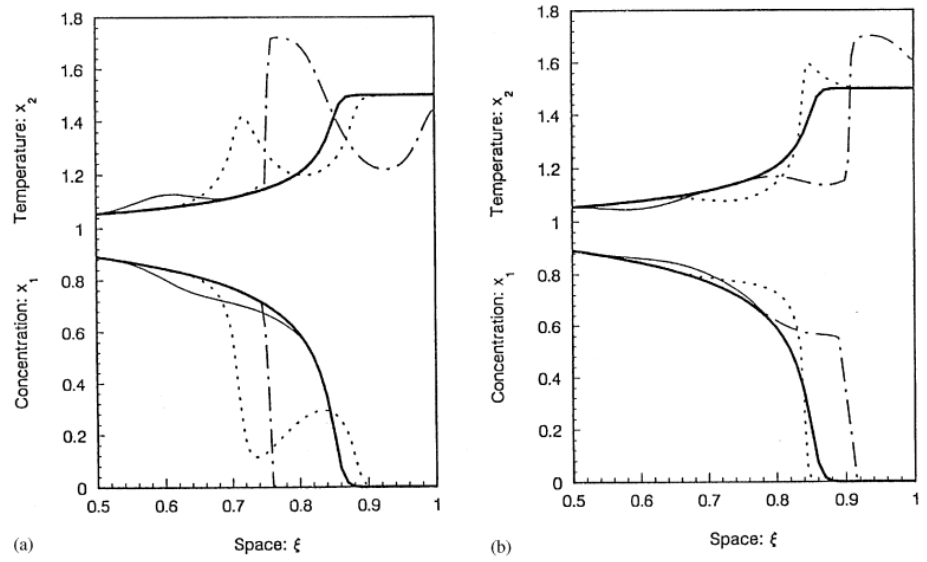

Figure 3.2: Waves of concentration and temperature, evolving from a (a) positive and (b) negative perturbation of the reactor inlet temperature. The perturbation is a single positive or negative half-period of a harmonic oscillation with frequency $\nu = 1.2$ and amplitude $a = 0.01$. The parameters have the values $Pe_m = 3000$, $Pe_h = 1000$, $Le = 3$, $\beta = 0.5$, $Da = 0.135$, $\gamma = 22$. The figure is from [4].

The plot also shows three other lines. These are snapshots of the concentration and temperature profiles at different times after a small perturbation has been applied to the inlet temperature. The thin solid lines correspond to $t = 2$, the dotted lines to $t = 2.5$, while the dash-dotted lines correspond to $t = 2.9$. In the left figure, a positive perturbation creates a temperature wave, which then generates a negative wave of concentration. The higher velocity of matter flow then generates a phase-shift between the two waves and this results in moving hot spots. Note that the temperature wave is negative compared to the steady state when it reaches the end of the reactor. This is a phenomenon known as wrong-way behaviour. In the right figure, a negative perturbation on the inlet temperature also gives rise to a moving hot spot. When this reaches the end of the reactor, the wave is positive compared to the steady

state so this is another example of wrong-way behaviour.
It is assumed in [4] that there is no heat transfer between the reaction mixture and the reactor wall, i.e. that $y_{2w} = y_2$.

The question of uniqueness of the solution is addressed in [5]. It is described that, for the solution to be unique in the general case with uneven Peclet numbers for mass and heat, it is sufficient to have high values of the Peclet numbers or small values of the Damköhler number. On the other hand, higher values of the dimensionless adiabatic temperature rise and the dimensionless activation energy enlarge the region of multiplicity, although more than three steady states are only possible for the non-adiabatic case.
A discussion of how to discretize the system is also contained in [5]. Different methods are discussed and the method of orthogonal spline collocation is recommended. Finite difference methods are actually ruled out as they require a lot of mesh points for stiff problems. It should be noted that [5] was published in 1982, where memory issues and computational time were greater challenges than today. Therefore, finite difference will be used in this report as it is a lot simpler to implement than orthogonal spline collocation and does no longer cause problems with memory and computational time. An actual bifurcation analysis is also performed in [5] with respect to the Damköhler number. All of the results will not be shown here, but a bifurcation diagram for the concentration can be seen in figure 3.3. The diagram shows two limit point bifurcations, which are denoted turning points in both the article and the diagram. There are no units on the axis so it is not possible to tell exactly where these bifurcations occur. The diagram is created with the parameter values

$$Pe_m = 320,\ Pe_h = 100,\ \beta = 0.994,\ \gamma = 16.9,\ y_{2w} = 1.57,\ H_w = 0.72. \tag{3.1}$$

It is also explained which methods are used to obtain these diagrams but this will not be handled here as it is not relevant to this report. For additional techniques for bifurcation analysis and classification of steady states, see [9].

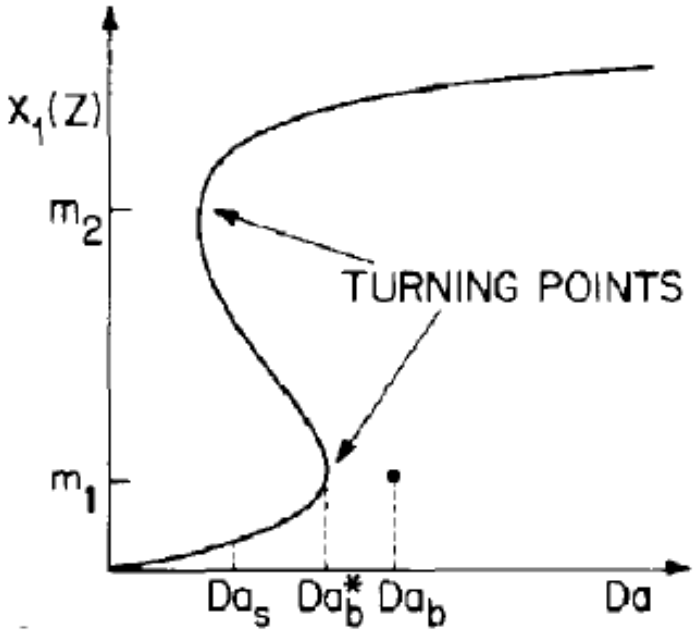

Figure 3.3: Concentration for varying Da. The parameters have the values $Pe_m = 320$, $Pe_h = 100$, $\beta = 0.994$, $\gamma = 16.9$, $y_{2w} = 1.57$, $H_w = 0.72$. The figure is from [5].

Chapter 4

Model Discretization and Validation

In order to be able to do any analysis of the model, it has to be discretized and implemented in MatLab. To do this, the method of lines discretization will be used. This is a semi-discrete finite difference method as it only discretizes the equations in space but not in time. The output of this method is a system of ordinary differential equations (ODE's), which can then be solved using the MatLab function `ode15s`, that is designed to solve stiff problems. To begin with, the discretization will be done without the term describing heat transfer between the reaction mixture and the reactor wall, i.e. it is assumed that $y_{2w} = y_2$. This is done so that it is possible to compare the results to the ones from [4]. The heat transfer term will then be added afterwards.

4.1 Model Discretization without Heat Transfer

At first, the equation (2.25) will be discretized. The first order derivative $\partial Y_1^j/\partial x$ will be replaced by the approximation

$$D_x Y_1^j = \frac{-1}{2h}\left(Y_1^{j+1} - Y_1^{j-1}\right),$$

where Y_1^j is the function value $y_1(x_j)$, where $x_j = jh$. Here, j is the grid point number and $h = 1/(m+1)$ is the mesh width. m is the number of grid points and D_x is the derivative operator. The second order derivative will be replaced by the approximation

$$D_x^2 Y_1^j = \frac{1}{h^2}\left(Y_1^{j-1} - 2Y_1^j + Y_1^{j+1}\right).$$

These approximations have been derived in [3]. The first equation ($j = 1$) involves the function value at $x = 0$, i.e. Y_1^0, and the last equation ($j = m$) involves the function value at $x = 1$, i.e. Y_1^{m+1}. As the function values at the boundaries are not given they need to be approximated. The derivative at the inlet boundary can be approximated to second order using the approximation

$$D_x Y_1^0 = \frac{1}{h}\left(\frac{3}{2}Y_1^0 - 2Y_1^1 + \frac{1}{2}Y_1^2\right)$$

derived in [3]. Inserting this approximation in (2.28) yields

$$\begin{aligned}&\frac{1}{h}\left(\frac{3}{2}Y_1^0 - 2Y_1 + \frac{1}{2}Y_1^2\right) + Pe_m y_1\left(0^-, t\right) - Pe_m Y_1^0 = 0 \quad \Leftrightarrow \\ &Y_1^0 = \frac{2Pe_m h y_1\left(0^-, t\right) - 4Y_1^1 + Y_1^2}{2Pe_m h - 3}.\end{aligned}$$

The derivative at the exit boundary is approximated by

$$D_x Y_1^{m+1} = \frac{1}{h}\left(\frac{3}{2}Y_1^{m+1} - 2Y_1^m + \frac{1}{2}Y_1^{m-1}\right).$$

Inserting this in (2.30) and solving for Y_1^{m+1} makes the approximation to the function value at the exit boundary

$$Y_1^{m+1} = \frac{1}{3}\left(4Y_1^m - Y_1^{m-1}\right).$$

Using this approach, the equation (2.25) can be written as

$$Y_1' = \left(A_1 + B_1 + C_1\right) Y_1 + G_1, \tag{4.1}$$

where A_1 is a diagonal matrix with $-Da\exp(\gamma(1 - 1/Y_2^j))$ in the jth diagonal element and

$$B_1 = \frac{1}{Pe_m}\frac{1}{h^2}\begin{bmatrix} -2 & 1 & & & & \\ 1 & -2 & 1 & & & \\ & 1 & -2 & 1 & & \\ & & \ddots & \ddots & \ddots & \\ & & & 1 & -2 & 1 \\ & & & & 1 & -2 \end{bmatrix}, \qquad C_1 = -\frac{1}{2h}\begin{bmatrix} 0 & 1 & & & & \\ -1 & 0 & 1 & & & \\ & -1 & 0 & 1 & & \\ & & \ddots & \ddots & \ddots & \\ & & & -1 & 0 & 1 \\ & & & & -1 & 0 \end{bmatrix}.$$

Finally

$$Y_1 = \begin{bmatrix} Y_1^1 \\ Y_1^2 \\ \vdots \\ Y_1^{m-1} \\ Y_1^m \end{bmatrix}, \qquad G_1 = \begin{bmatrix} \left(\frac{1}{Pe_m}\frac{1}{h^2} + \frac{1}{2h}\right) Y_1^0 \\ 0 \\ \vdots \\ 0 \\ \left(\frac{1}{Pe_m}\frac{1}{h^2} - \frac{1}{2h}\right) Y_1^{m+1} \end{bmatrix}.$$

As $A_1, B_1, C_1 \in \mathbb{R}^{m\times m}$ and $Y_1, G_1 \in \mathbb{R}^m$, this is a system of m ODE's.
The equation (2.26) is discretized in an equivalent way and can be written as

$$Y_2' = \frac{1}{Le}\left(A_2 Y_1 + (B_2 + C_2)\, Y_2 + G_2\right), \tag{4.2}$$

where A_2 is a diagonal matrix with $Da\beta \exp(\gamma(1 - 1/Y_2^j))$ in the jth diagonal element and

$$B_2 = \frac{1}{Pe_h}\frac{1}{h^2}\begin{bmatrix} -2 & 1 & & & & \\ 1 & -2 & 1 & & & \\ & 1 & -2 & 1 & & \\ & & \ddots & \ddots & \ddots & \\ & & & 1 & -2 & 1 \\ & & & & 1 & -2 \end{bmatrix}.$$

Furthermore $C_2 = C_1$ and

$$G_2 = \begin{bmatrix} \left(\frac{1}{Pe_h}\frac{1}{h^2} + \frac{1}{2h}\right) Y_2^0 \\ 0 \\ \vdots \\ 0 \\ \left(\frac{1}{Pe_h}\frac{1}{h^2} - \frac{1}{2h}\right) Y_2^{m+1}. \end{bmatrix},$$

while Y_2 is built up in the same way as Y_1. This is also a system of m ODE's which means that $2m$ ODE's need to be solved in order to simulate the entire system.
The MatLab implementation of the system can be seen in appendix A.1. The MatLab script that actually solves this system can be found in appendix A.2. This script simulates the system for different times and the resulting dimensionless concentration and temperature profiles can be seen in figure 4.1a and 4.2a respectively. All of the simulations in this chapter have been done with the parameter values

$$Pe_m = 3000, \quad Pe_h = 1000, \quad Le = 3, \quad \beta = 0.5, \quad Da = 0.135, \quad \gamma = 22.$$

The dimensionless concentration profiles in figure 4.1a show that, for times $\tau = 2$ and $\tau = 3$, some of the reactant is actually leaving the reactor. This is usually not the case as the reaction normally has the form

$$A \longrightarrow B,$$

meaning that all of the reactant is used in the reaction and only B will exit the reactor. The reason for this behaviour is the low Damköhler number, $Da = 0.135$, which corresponds to a low kinetic reaction rate or a low residence time, i.e. high gas velocity. The script also produces three-dimensional plots with both time and length as the independent variables. These can be seen in figure 4.1b and 4.2b. Here one can see the development of the profiles over time and that the system reaches a steady state around $\tau = 4$.

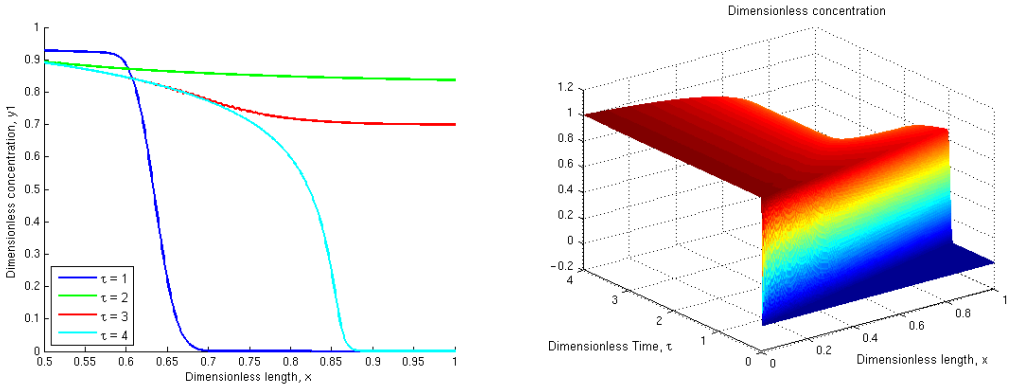

(a) (b)

Figure 4.1: Simulations of the dimensionless concentration. (a) shows the dimensionless concentration as a function of length for different times and (b) shows the dimensionless concentration as a function of both length and time.

To validate that the implementation is correct, this simulated steady state will be compared to the simulation of the steady state presented in [4], which can be seen in figure 3.2. The data has been retrieved from the article using the program Engauge Digitizer [11], then interpolated using MatLab's `interp1` function and finally plotted together with the simulated steady states for both dimensionless concentration and temperature. This can be seen in figure 4.3 and 4.4 respectively. The same steady states seem to have been found, which means that the discrtization must be correct. This is also confirmed by the residual plots in figure 4.3 and 4.4.

Some small irregularities are observed here though, but these are most likely caused by differences in the numerical method. It is not specified which numerical method is used in [4] but it is most likely not the same as the one used in this report. Hence, it will be assumed

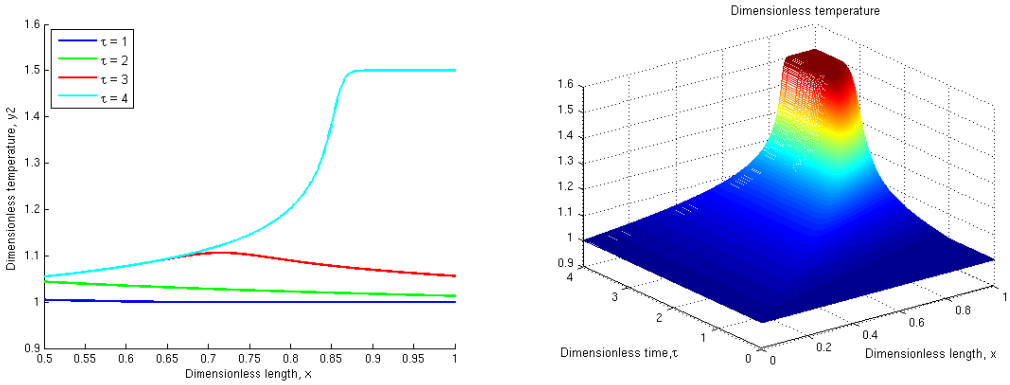

(a) (b)

Figure 4.2: Simulations of the dimensionless temperature. (a) shows the dimensionless temperature as a function of length for different times and (b) shows the dimensionless temperature as a function of both length and time.

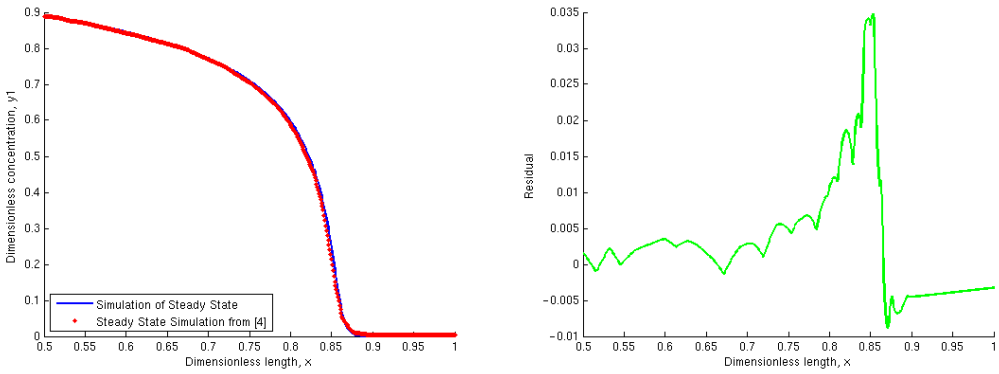

(a) (b)

Figure 4.3: Comparison of the simulation of the steady state of dimensionless concentration to the steady state from [4]. (a) The two steady states plotted together. (b) The residual plot.

that the discretization is correct.

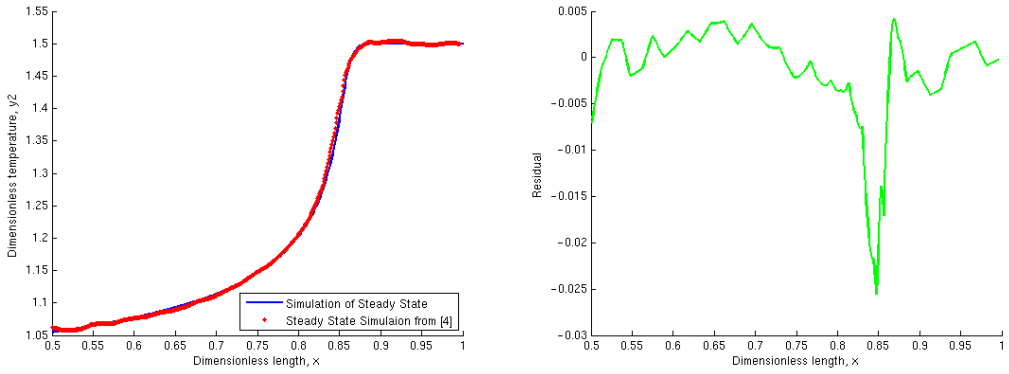

(a) (b)

Figure 4.4: Comparison of the simulation of the steady state of dimensionless temperature to the steady state from [4]. (a) The two steady states plotted together. (b) The residual plot.

4.2 Model Discretization with Heat Transfer

The term that describes the heat transfer between the reaction mixture and the reactor wall is now added. The system of equations describing the concentration dynamics stays the same, while the system for the temperature takes the form

$$Y_2' = \frac{1}{Le}\left(A_2 Y_1 + \left(B_2 + C_2 + H_2\right) Y_2 + G_2 + W_2\right), \tag{4.3}$$

where

$$H_2 = \begin{bmatrix} -H_w & & \\ & \ddots & \\ & & -H_w \end{bmatrix} \quad \text{and} \quad W_2 = \begin{bmatrix} H_w y_{2w} \\ \vdots \\ H_w y_{2w} \end{bmatrix}.$$

The complete implementation of the system can be seen in appendix A.3. Simulations of the concentration and temperature are then done. The results can be seen in figure 4.5 and 4.6. The dimensionless heat transfer coefficient is set to $H_w = 0.5$ and the dimensionless wall temperature is set to $y_{2w} = 1$. Comparing figure 4.6 and figure 4.2 show that the outlet temperature in the steady state is lower when heat transfer is assumed. This is because the wall temperature is relatively low and this then lowers the temperature of the reaction mixture in the reactor.

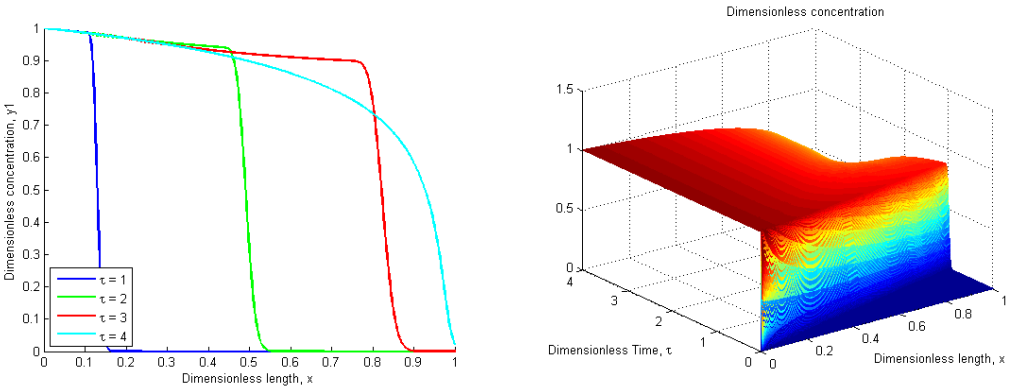

(a) (b)

Figure 4.5: Simulations of the model with heat transfer between the reaction mixture and the reactor wall. The dimensionless wall temperature is $y_{2w} = 1$. (a) shows the development in dimensionless concentration over time and (b) shows dimensionless concentration profiles for different times.

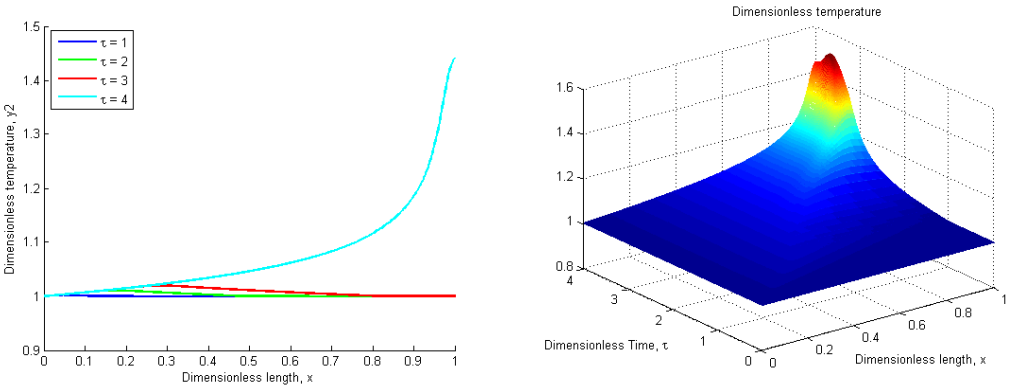

(a) (b)

Figure 4.6: Simulations of the model with heat transfer between the reaction mixture and the reactor wall. The dimensionless wall temperature is $y_{2w} = 1$. (a) shows the dimensionless temperature development over time and (b) shows dimensionless temperature profiles for different times.

Chapter 5

Model Analysis

When the model has been implemented in MatLab, the system can be analysed further. It will be investigated how the system reacts to process disturbances as this is a real threat that can cause great problems. Furthermore an analysis of the effect of the many parameters will be done.

5.1 Convective Instability

In the previous chapter, the plots were created under the assumption that the concentration- and temperature of the gas at the inlet boundary were $c = c_0$ and $T = T_0$ respectively. This then made $y_1(0^-, t) = c/c_0 = 1$ and $y_2(0^-, t) = T/T_0 = 1$ and this was used as arguments for the function in appendix A.1. It is now investigated how the system reacts to process disturbances in the form of a step change of -5% in the inlet temperature. This is done using the script from appendix A.4. Here the steady state from before is found and used as an initial condition and then the step change is added after some time. This means that the value of $y_2(0^-, t)$ is changed from 1 to 0.95. The model is then simulated until the system reaches a new steady state. The resulting temperature distribution can be seen in figure 5.1. This figure shows that a moving hot spot occurs after the step change has been applied, which means that the system shows convectively unstable behaviour as expected. The hot spot has a maximum temperature of $y_{2max}(x, t) = 1.8$, while the maximum temperature of the steady state is $y_{2ss} = 1.5$. This means that a 5% decrease in the inlet temperature yields a 20% increase in the outlet temperature! This is an example of wrong-way behaviour as explained

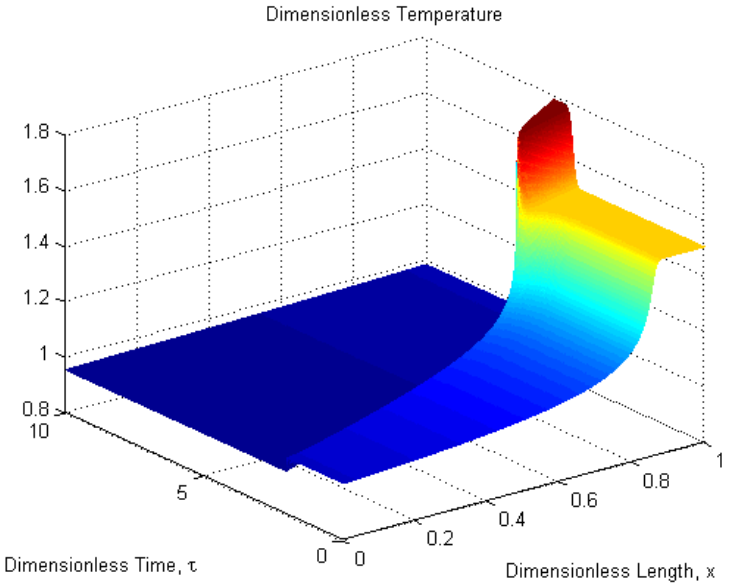

Figure 5.1: The dimensionless temperature as a function of length and time. The parameter values are $Pe_m = 3000$, $Pe_h = 1000$, $Le = 3$, $\beta = 0.5$, $Da = 0.135$, $\gamma = 22$.

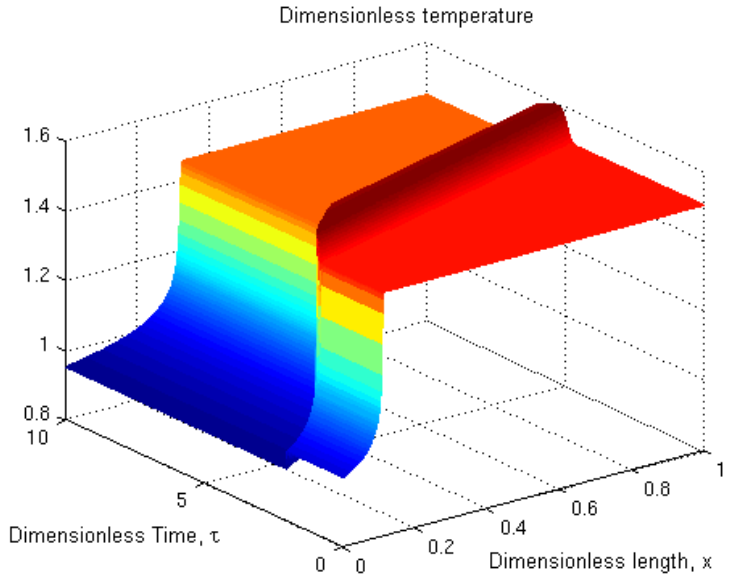

Figure 5.2: The dimensionless temperature as a function of length and time. The parameter values are $Pe_m = 3000$, $Pe_h = 1000$, $Le = 3$, $\beta = 0.5$, $Da = 1$, $\gamma = 22$.

in chapter 3. After the temperature wave is washed out, the reaction suddenly extinguishes. This is because of the very low value of the Damköhler number, $Da = 0.135$. Normally in the chemical industry, catalysts would not operate under such conditions so the reaction would normally not extinguish like this. With a higher Damköhler number, e.g. $Da = 1$, the reaction does not extinguish after the hot spot has occurred, see figure 5.2.
The simulations show that the packed-bed reactor works as an amplifier of process disturbances. This is a limited problem for the packed-bed reactor itself but it can pose a big problem when integrated with a heat exchanger, see chapter 7.

5.2 Parameter Effects

This section will investigate the effects of the different parameters in the packed-bed reactor model. The theoretical implications of changes in the parameter values will be presented

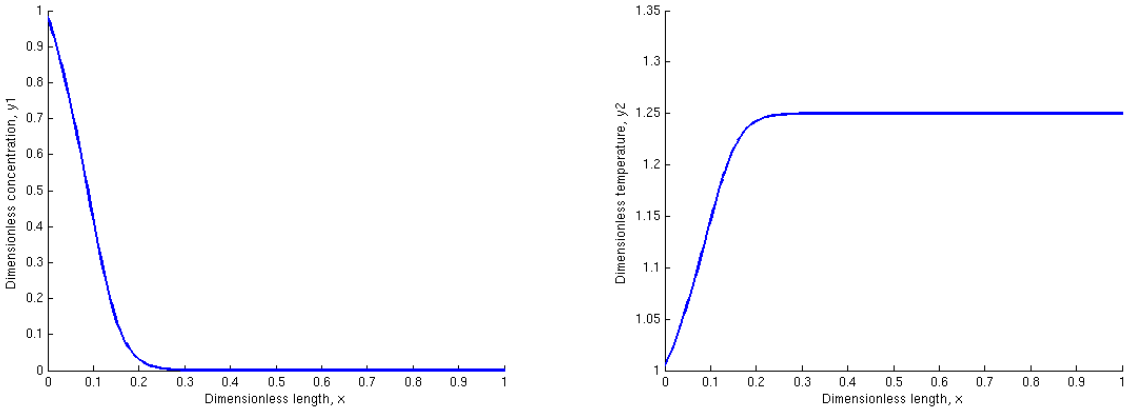

(a) The dimensionless concentration.

(b) The dimensionless temperature.

Figure 5.3: Dimensionless concentration- and temperature steady states for the parameter values (5.1).

and compared to results from simulations of the steady state. To do these simulations, the parameters will initially have the values

$$Da = 4, \quad Le = 40, \quad \gamma = 11, \quad \beta = 0.25, \quad Pe_m = 1000, \quad Pe_h = 1000 \tag{5.1}$$

and then they will be changed one at a time to see how each change affects the steady state of the system. The steady state of the system with these parameters can be seen in figure 5.1. The ranges of the parameters that will be investigated can be seen in table 5.1. These ranges have been chosen so that they are representative for many different processes in the chemical industry. For the first 6 parameters, the simulations will be done under the assumption that there is no heat transfer between the reaction mixture and the reactor wall.

Parameter	Minimum Value	Maximum Value
Da	0.1	50
Le	20	100
γ	10	40
β	0.1	0.5
Pe_h	10	1000
Pe_m	10	1000

Table 5.1: The parameter space.

5.2.1 The Damköhler Number, Da

In section 2.4, the Damköhler number was defined as the kinetic reaction rate to the rate of transport by convection at the entrance of the reactor, i.e.

$$Da = \frac{(1-\epsilon_B)\, Lk_0}{v_z} e^{-\gamma}. \tag{5.2}$$

Another way of defining the Damköhler number is as the kinetic reaction rate times the residence time. The reaction rate is defined as $k_0' = k_0 e^{-\gamma}$, while the residence time is $\tau_r = (1-\epsilon_B)\, L/v_z$. This is an expression of the average amount of time a particle spends in the reactor. The Damköhler number can then be written as

$$Da = k_0' \tau_r.$$

Both these representations of the Damköhler number show that a higher reaction rate results in a higher Damköhler number. This means that the reaction will happen faster for high values of the Damköhler number.

To illustrate this, a simulation of the steady state is made. The Damköhler number is varied from one to 50, while all other parameter values are held constant. These steady state profiles can be seen in figure 5.4 and they confirm that the reaction happens faster for high values of Da. For $Da = 50$, the reaction happens very fast and the concentration of the reactant

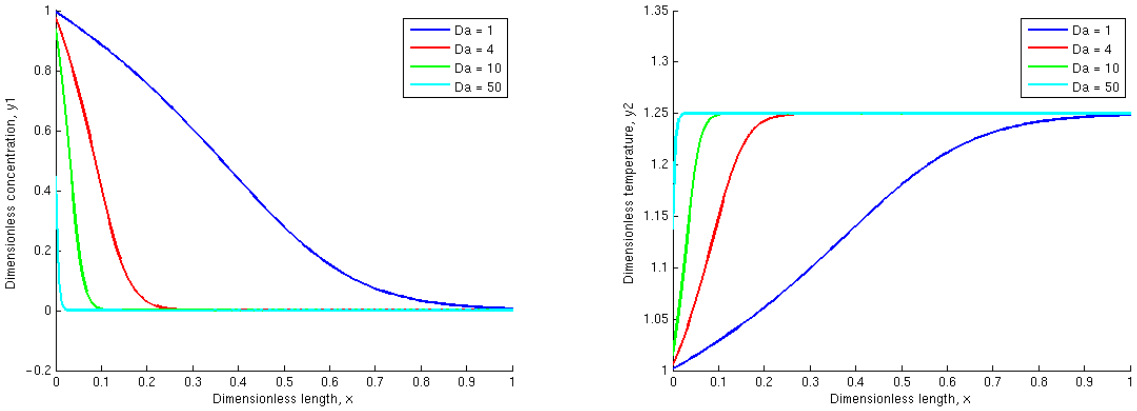

(a) The dimensionless concentration.

(b) The dimensionless temperature.

Figure 5.4: Dimensionless concentration- and temperature profiles of the steady state for varying values of Da.

quickly drops to zero, while the concentration only drops to zero at the end of the reactor for $Da = 1$, see figure 5.4a. The temperature rises equivalently as reactions happen faster at high temperatures, see figure 5.4b.

5.2.2 The Lewis Number, Le

The Lewis number was previously defined as the ratio of the thermal transport time constant to the material transport time constant, i.e.

$$Le = \frac{(\epsilon_B \rho_g C_{pg} + (1 - \epsilon_B)\, \rho_s C_{ps})}{\epsilon_B \rho_g C_{pg}}.$$

This number is usually used to describe fluid flows with both heat- and mass transfer by convection. As described in chapter 3, the velocity of matter flow will always be greater than the velocity of heat flow as the second model equation is scaled by Le^{-1}, which is always smaller than 1. Decreasing Le towards one will then increase the scale factor, Le^{-1}, and make the temperature grow faster. As a consequence, the concentration will drop faster for

small values of Le. To verify this, simulations of the concentration- and temperature profiles are done. Changes in the Lewis number will have no effect on the steady state of the system as it only appears on the left-hand side of equation (2.26) and the simulations will therefore be done for time $\tau = 3$ instead. This is the only parameter that will not be analysed in the steady state. The profiles can be seen in figure 5.5 and they confirm the expected behaviour.

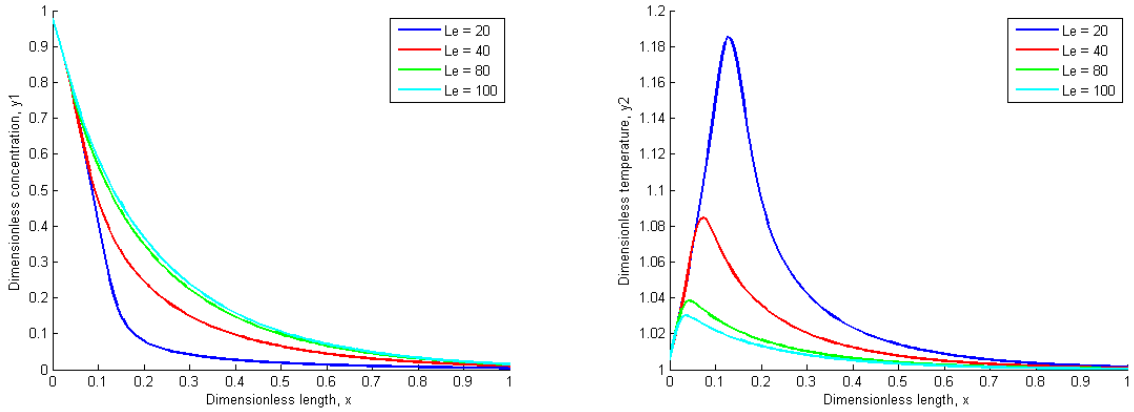

(a) The dimensionless concentration.

(b) The dimensionless temperature.

Figure 5.5: Dimensionless concentration- and temperature profiles at time $\tau = 3$ for varying values of Le.

5.2.3 The Dimensionless Activation Energy, γ

The dimensionless activation energy is defined as

$$\gamma = \frac{E_a}{RT_0}.$$

Unlike all the other parameters, one cannot obtain a correct picture of the effect of γ just by changing it and keeping the other parameters constant. This is because γ is also a part of the definition of Da, see (5.2). Therefore the value of Da is set to $4/e^{-\gamma^*}$, where γ^* is the initial value of γ. Furthermore the factor $e^{-\gamma^*}$ is multiplied to the exponential term in the system equations. Thereafter γ is changed as usual. The result can be seen in figure 5.6. From this figure it can be seen that the reaction happens slower for high values of γ. This is because more energy is needed for the reaction to take place in this situation.

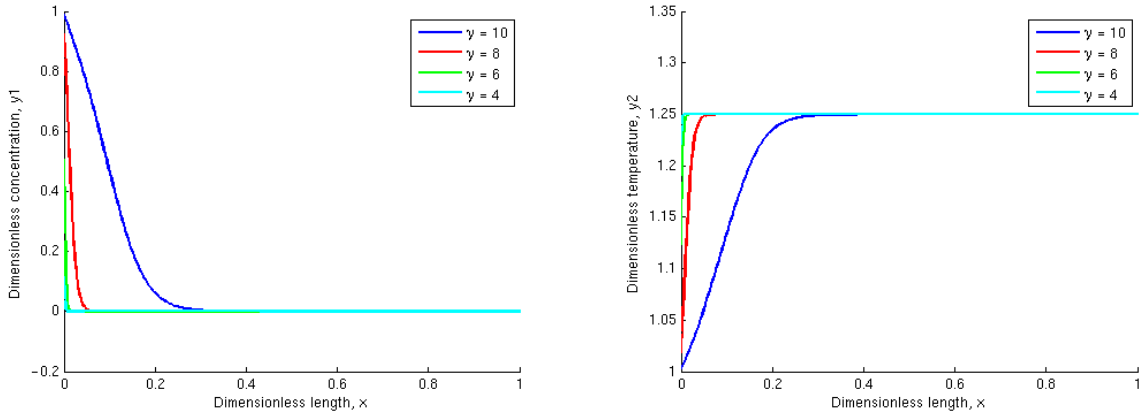

(a) The dimensionless concentration.

(b) The dimensionless temperature.

Figure 5.6: Dimensionless concentration- and temperature profiles of the steady state for varying values of γ.

5.2.4 The Dimensionless Adiabatic Temperature Rise, β

The dimensionless adiabatic temperature rise is defined as

$$\beta = \frac{(-\Delta H)c_0}{\rho_g C_{pg} T_0},$$

which means that β rises with the change in reaction enthalpy. Because the reaction is exothermic, the change is negative. The larger the factor $-\Delta H$, the more energy is released and hence the temperature will rise. This can be confirmed by examining figure 5.7. As expected, the temperature of the reactant rises with β, see figure 5.7b. The corresponding concentration then drops faster as reactions happen faster at high temperatures, see figure 5.7a.

5.2.5 The Peclet Number for Heat, Pe_h

The Peclet number for heat was previously defined as the ratio of the rate of transport of heat by convection to the rate of transport of heat by dispersion. The rate of dispersion will therefore get higher for $Pe_h \to 0$. This should create more even temperature profiles throughout the reactor as the heat gets mixed better for low values of Pe_h. This behaviour is really hard to realize as it is not possible to find the steady state for $Pe_h <\sim 250$. The

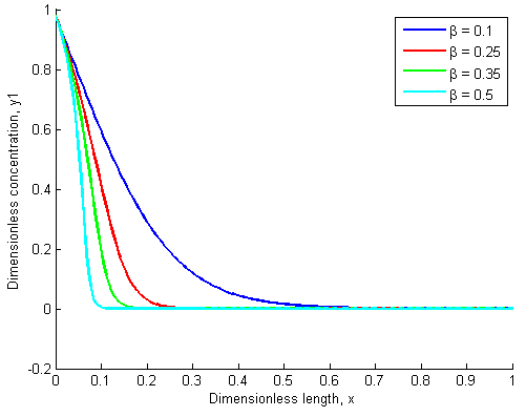

(a) The dimensionless concentration.

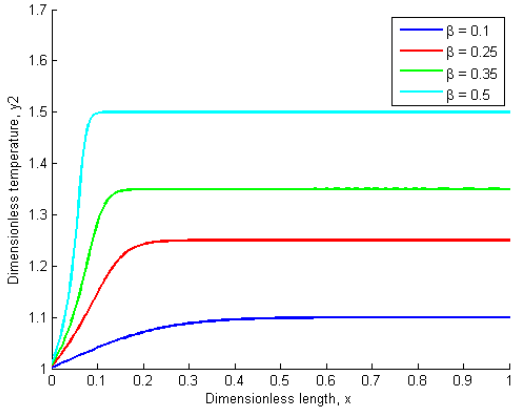

(b) The dimensionless temperature.

Figure 5.7: Dimensionless concentration- and temperature profiles of the steady state for varying values of β.

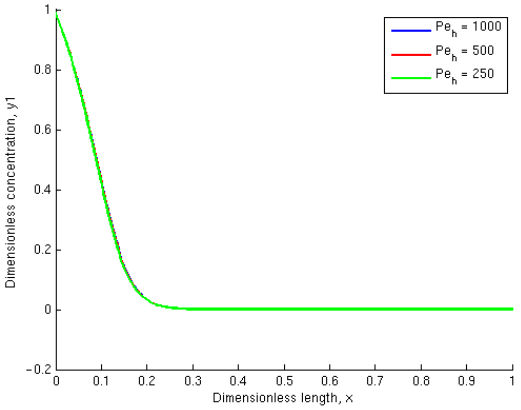

(a) The dimensionless concentration.

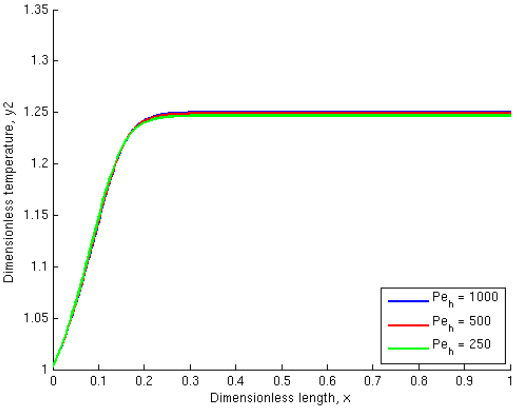

(b) The dimensionless temperature.

Figure 5.8: Dimensionless concentration- and temperature profiles of the steady state for varying values of Pe_h.

solution simply diverges for low values of Pe_h, most likely because of the method of lines discretization. This does however not pose a problem as most industrial reactors operate with $Pe_h \sim 10^3$. With these high values of Pe_h the dispersion effect is very little so it is hard to see any changes in the profiles, see figure 5.8. By zooming in on the area around $x = 0$,

see figure 5.9, one can see that the profiles are actually getting more even as the curves rise a bit for lower values of Pe_h.

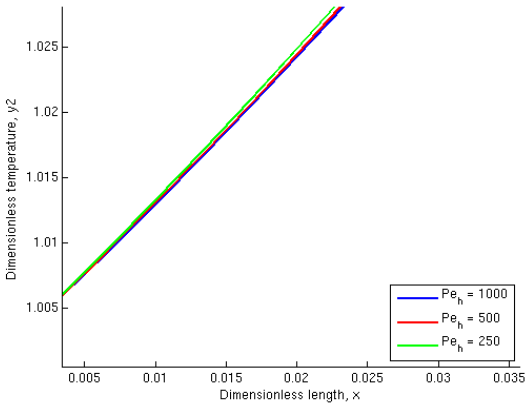

Figure 5.9: Dimensionless temperature profiles of the steady state near the inlet for varying values of Pe_h.

5.2.6 The Peclet Number for Mass, Pe_m

Similarly to Pe_h, the Peclet number for mass is defined with mass instead of heat. This means

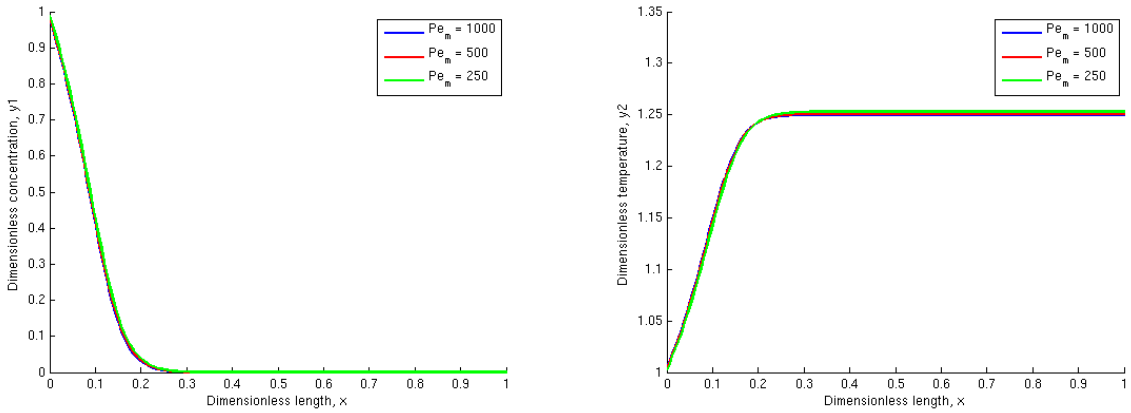

(a) The dimensionless concentration.

(b) The dimensionless temperature.

Figure 5.10: Dimensionless concentration- and temperature profiles of the steady state for varying values of Pe_m.

that low values of Pe_m are induced by a high dispersion rate, which makes the concentration profiles more even throughout the reactor. Again, it is not possible to find the steady state for $Pe_m <\sim 250$ with this discretization scheme and it is therefore only possible to see very small changes in the profiles. The profiles can be seen in figure 5.10.

5.2.7 The Dimensionless Overall Heat Transfer Coefficient

In the following it is assumed that there is heat transfer between the reaction mixture and the reactor wall, i.e. that $y_2 \neq y_{2w}$. This means that the term including the dimensionless overall heat transfer coefficient now plays a role. The dimensionless heat transfer coefficient was defined as the reciprocal of the sum of the resistances to the heat transfer. The resistance to heat transfer is primarily in the form of a film near the reactor wall. The thermal conductivity of this film is therefore crucial to the effect of heat transfer. If it is high, the resistance becomes smaller and the dimensionless overall heat transfer coefficient then becomes higher. This means that heat is easily transferred between the reaction mixture and the reactor wall for high values of H_w and that the film works as isolation for low values of H_w. This can be confirmed by figure 5.11, which shows the steady state profiles of the concentration and the temperature for different values of H_w. In this figure the dimensionless wall temperature is chosen as $y_{2w} = 1$. Here it is seen that the steady states of the concentration- and temperature

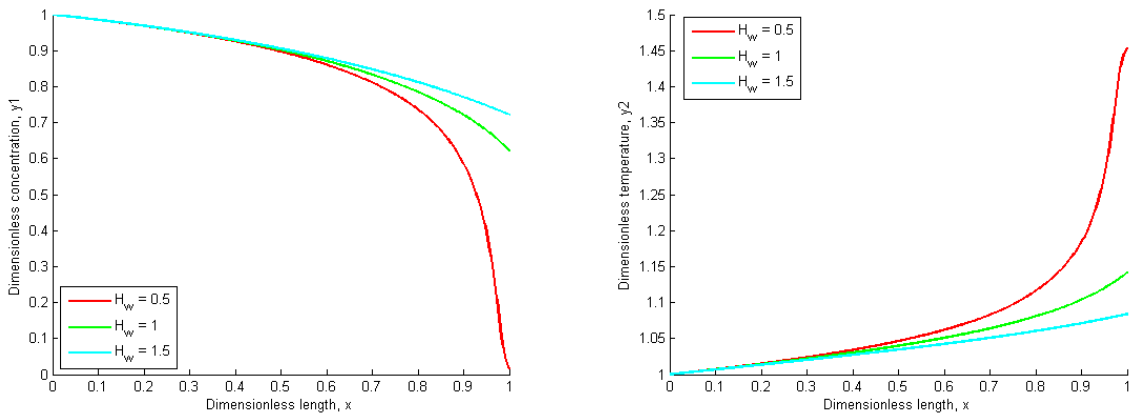

(a) The dimensionless concentration.

(b) The dimensionless temperature.

Figure 5.11: Dimensionless concentration- and temperature profiles of the steady state for varying values of H_w.

profiles become more affected by the wall temperature when $H_w \to \infty$ and that these profiles approach the steady states from figure 4.5a and 4.6a when $H_w \to 0$. The reason that outlet temperatures drops for high values of H_w is that $y_{2w} = 1$. This is a relatively low temperature compared to the outlet temperature and this then cools the reaction mixture down.

5.2.8 The Dimensionless Wall Temperature

As the wall is heated up, i.e. when y_{2w} grows, the reaction mixture will get warmer and this will then make the concentration of the reactant drop faster towards zero. This can be verified by figure 5.12, which shows the steady state profiles of the concentration and the temperature for different values of y_{2w}. The dimensionless overall heat transfer coefficient is chosen as $H_w = 0.5$.

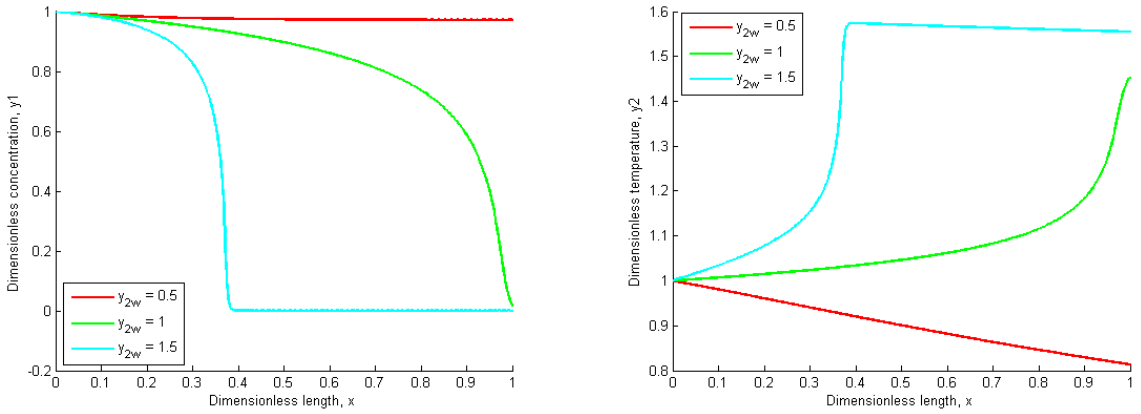

(a) The dimensionless concentration.

(b) The dimensionless temperature.

Figure 5.12: Dimensionless concentration- and temperature profiles of the steady state for varying values of y_{2w}.

Chapter 6

Bifurcation Analysis of the Reactor Model

In this chapter, bifurcation analysis will be performed on the packed-bed reactor model in order to obtain more knowledge of the system. This includes learning which parameters affect the steady state most and to see if any bifurcations are present in the given parameter space. The analysis is done on the model without heat transfer to the reactor wall as this has very little effect on the bifurcation diagrams.

6.1 Bifurcation Theory

A dynamical system can in general be written in the form

$$\begin{aligned} \dot{x}_1 &= f_1(x_1, \ldots, x_n, \mu) \\ &\vdots \\ \dot{x}_n &= f_n(x_1, \ldots, x_n, \mu), \end{aligned} \tag{6.1}$$

where $n \in \mathbb{N}$ is the dimension of the system, $f_1, \ldots, f_n$ are given functions and $\mu \in \mathbb{R}^m$ is a vector of parameters. Note that this is also the case for systems of ODE's with order higher than one. These can always be written in the form (6.1) by introducing new variables.
As parameters are varied, qualitative changes in the dynamics can occur. This can be in the form of change in stability of fixed points or creation or destruction of fixed points. These qualitative changes in the dynamics are called bifurcations. The parameter values for which

these changes happen are called bifurcation points.

These changes in dynamics are conventionally illustrated in bifurcation diagrams, where the fixed points can be seen as a function of an active parameter.

To determine whether a fixed point is stable or not for a given parameter value one can either examine the vector field of the system or the eigenvalues of the Jacobian, J, of the system. For a nonlinear system, a fixed point, x_s, is unstable if $J(x_s)$ has an eigenvalue with positive real part and x_s is stable if all of the eigenvalues have negative real part, see [17].

When a fixed point is stable, there are two ways it can loose its stability. First, a real eigenvalue can cross the imaginary axis from left to right. This gives rise to a limit point bifurcation. These can occur when two different steady states, one stable and one unstable, coexist for some value of the parameter. When the parameter value is varied, the two states move towards each other and finally collide. When this happens it is said that a limit point bifurcation has occurred. If the parameter is varied further in the same direction, the steady states mutually annihilate.

Second, two complex conjugate eigenvalues can cross the imaginary axis simultaneously from left to right, which gives rise to a Hopf bifurcation that causes oscillations of the solution. Hopf bifurcations can come in both super- and subcritical varieties.

Suppose that a disturbance is washed out through exponentially damped oscillations for some value of a parameter κ. If the oscillations start to grow when the parameter reaches some value κ_c, the system has undergone a supercritical Hopf bifurcation. Often, this results in small-amplitude oscillations around the former steady state. In the phase plane this can be seen as a stable spiral that changes to an unstable spiral surrounded by a limit cycle when κ crosses a critical parameter value κ_c. The behaviour of the subcritical Hopf bifurcation will not be presented here as it is not relevant to this report. For an elaboration of the different kinds of bifurcations, consult [16].

Even though the analysis of the eigenvalues can tell when a Hopf bifurcation occurs it cannot tell if the bifurcation is supercritical or subcritical. A complex pair of eigenvalues cross the imaginary axis in both cases. To determine the variety of the bifurcation one has to resort to other methods, as for instance computing and analysing the phase portrait.

The eigenvalues of the system do not only determine if, when and which bifurcations occur

but also how the solution looks. A linear system

$$\dot{x} = Ax, \tag{6.2}$$

where $A \in \mathbb{R}^{p\times p}$ and $x, \dot{x} \in \mathbb{R}^p$ has p eigenvalues, $\mu = a + ib$, and p eigenvectors, v, for which it holds that

$$Av = \mu v.$$

For each real eigenvalue with a corresponding real eigenvector the system has the solution

$$x = e^{\mu t}v$$

and for each complex pair of eigenvalues, with corresponding eigenvectors, the system has the solutions

$$x = \mathrm{Re}\left(e^{\mu t}v\right) = e^{at}\left(\cos\left(bt\right)\mathrm{Re}\left(v\right) - \sin\left(bt\right)\mathrm{Im}\left(v\right)\right)$$

and

$$x = \mathrm{Im}\left(e^{\mu t}v\right) = e^{at}\left(\sin\left(bt\right)\mathrm{Re}\left(v\right) + \cos\left(bt\right)\mathrm{Im}\left(v\right)\right)$$

according to [17]. The complete solution to the system is then a linear combination of the p found solutions with real coefficients. If the eigenvalues and eigenvectors are complex, the solution is a linear combination of terms of the type $e^{at}\cos\left(bt\right)$ and $e^{bt}\sin\left(bt\right)$. This means that if all of the eigenvalues have negative real part, the solution will consist of terms of exponentially damped oscillations and the fixed point will therefore be stable. On the other hand, if one eigenvalue has a positive real part, it will contribute to exponentially growing oscillations and the fixed point will therefore be unstable. Finally, the imaginary part determines the angular frequency of the oscillation.

This is although only directly applicable to linear systems but a nonlinear system will behave like its corresponding linear system in a small area around the fixed point, i.e. when disturbances are small enough.

6.2 MatCont

For models like the packed-bed reactor model, one needs to do bifurcation analysis through the use of some mathematical software. Several different pieces of bifurcation analysis software exist, like for instance Auto, Concent and MatCont. In this report MatCont will

be used, primarily because it is the only software that is compatible with the standard MATLAB representation of ODE's. MATCONT is open source software, available at [12].
The first thing to do, when doing bifurcation analysis in MATCONT, is to create a system file. This file contains the system definition and the initial conditions. The initial condition should be an approximative equilibrium solution to the system. Once this system file is created one has to choose initial values of the parameters, which MATCONT then will use to make its own simulation of the equilibrium solution. This will then work as the actual initial condition for the bifurcation analysis that is then performed. The output is a bifurcation diagram and a list of the locations of the detected bifurcations.
The algorithms in MATCONT are based on predictor-corrector methods. The details will not be presented here but one can consult the MATCONT manual, [15], for an elaborate explanation on the algorithms.

6.3 Analysis

In this section, the actual bifurcation analysis of the packed-bed reactor model will be performed. The parameters will initially have the values given by (5.1) and then they will be varied in the parameter space given by table 5.1 to see if any bifurcations occur in this space. The MATCONT system file used to perform this analysis can be seen in appendix A.5, while the script that actually creates the bifurcation diagrams can be seen in appendix A.6. Note that this script only performs the analysis with Da as the active parameter, but it can easily be adjusted to perform the analysis for any of the parameters. Bifurcation diagrams will be created for two different places in the reactor. First, they will be created for the spots in the reactor, where the concentration- and temperature fronts occur, i.e. where the profiles have the steepest gradient and second, for the end point of the reactor.
As previously mentioned Le has no effect on the steady state and a bifurcation analysis will therefore be indifferent. Instead, the analysis will start with Da.

6.3.1 The Damköhler Number, *Da*

Bifurcation diagrams for *Da* can be seen in figure 6.1 and 6.2 for the concentration and temperature respectively. The figures are in good correspondence with figure 5.4. The value

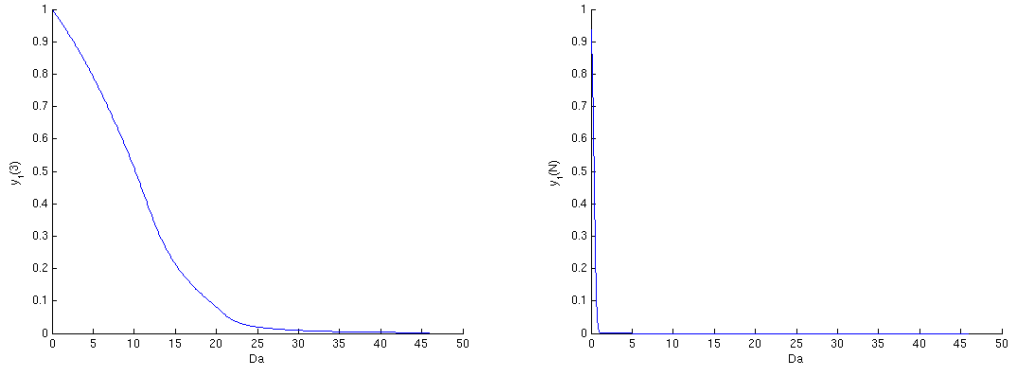

(a) (b)

Figure 6.1: Bifurcation diagram of the dimensionless concentration at (a) the front and (b) the endpoint. *Da* is the active parameter.

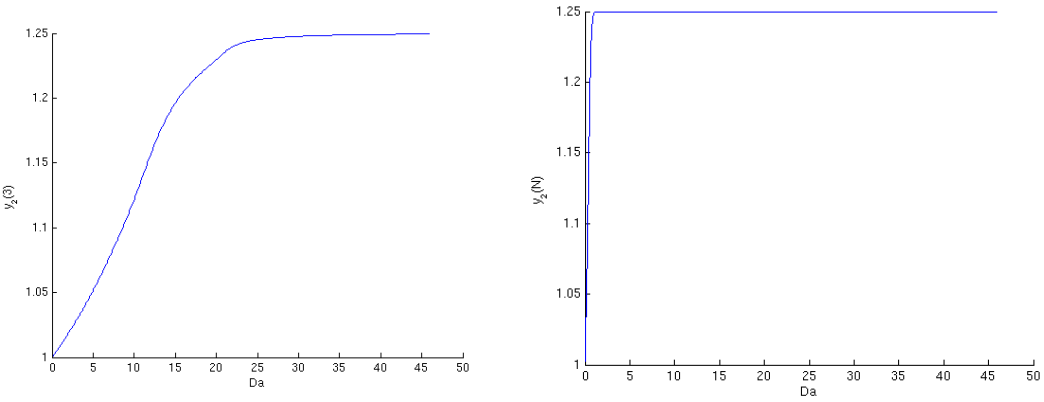

(a) (b)

Figure 6.2: Bifurcation diagram of the dimensionless temperature at (a) the front and (b) the endpoint. *Da* is the active parameter.

of the concentration in the first point is approximately 1 for $Da = 0$, while this value drops for higher values of *Da*. The temperature on the other hand grows for higher values of *Da*.

By examining the eigenvalues, it is found that they all have negative real part meaning that the steady states are stable. In the rest of this chapter, the analysis of the eigenvalues will not be mentioned so if nothing else is noted, it is because the steady states are stable.

6.3.2 The Dimensionless Activation Energy, γ

The bifurcation diagrams for γ can be seen in figure 6.3 and 6.4. No bifurcations were found here, but changes in γ affect the steady state as described earlier, i.e. by making the reaction occur at a slower rate for high values of γ. Once again, the diagrams are made for both the concentration- and temperature fronts and the end point of the reactor. It will be done this way for the rest of the section.

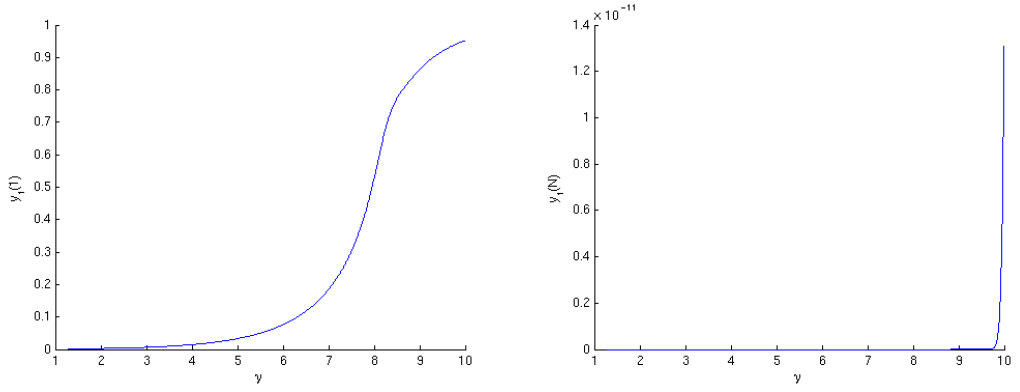

(a) (b)

Figure 6.3: Bifurcation diagram of the dimensionless concentration at (a) the front and (b) the endpoint. γ is the active parameter.

6.3.3 The Dimensionless Adiabatic Temperature Rise, β

The bifurcation diagrams for β can be seen in figure 6.5 and 6.6. Again no bifurcations are found, but the diagrams confirm the results found in section 5.2.4 regarding parameter dependency. Figure 6.5b and 6.6b show that the temperature in the end point rises with β, while the concentration falls accordingly. Figure 6.5a and 6.6a show that the front gets steeper for high values of β and this confirms the picture seen in figure 5.7.

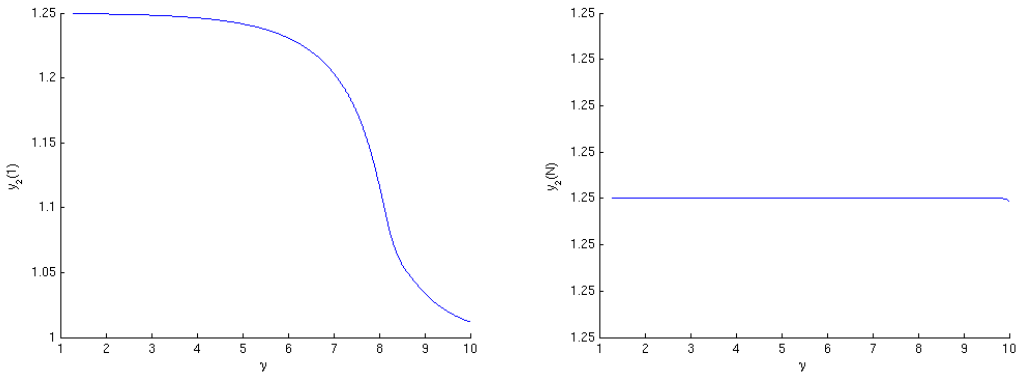

(a) (b)

Figure 6.4: Bifurcation diagram of the dimensionless temperature at (a) the front and (b) the endpoint. γ is the active parameter.

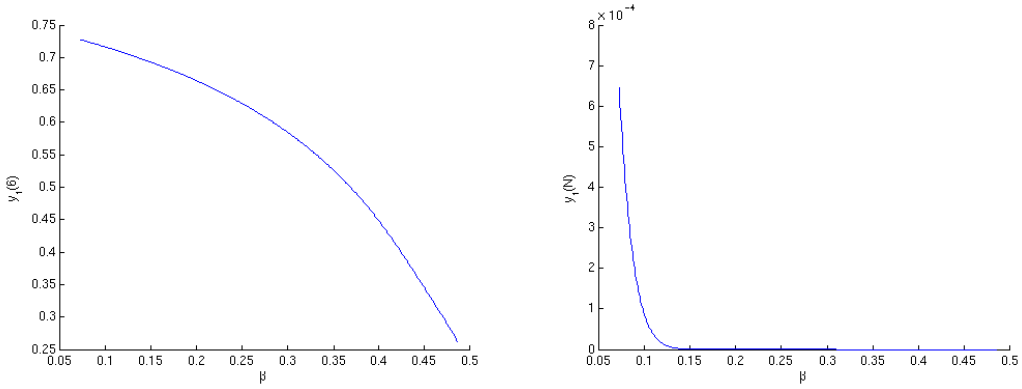

(a) (b)

Figure 6.5: Bifurcation diagram of the dimensionless concentration at (a) the front and (b) the endpoint. β is the active parameter.

6.3.4 The Peclet Number for Heat, Pe_h

The bifurcation diagrams for Pe_h can be seen in figure 6.7 and 6.8. From the y-axis it is clear that the changes in the steady states are quite small. This is because the values of Pe_h are so big that the effects of dispersion are quite small and the steady states will therefore look alike. This is confirmed by figure 5.8. When $Pe_h \to 0$ the dispersion effects get bigger and this can be confirmed by figure 6.7a and 6.8a, which show that the fronts rise a bit making

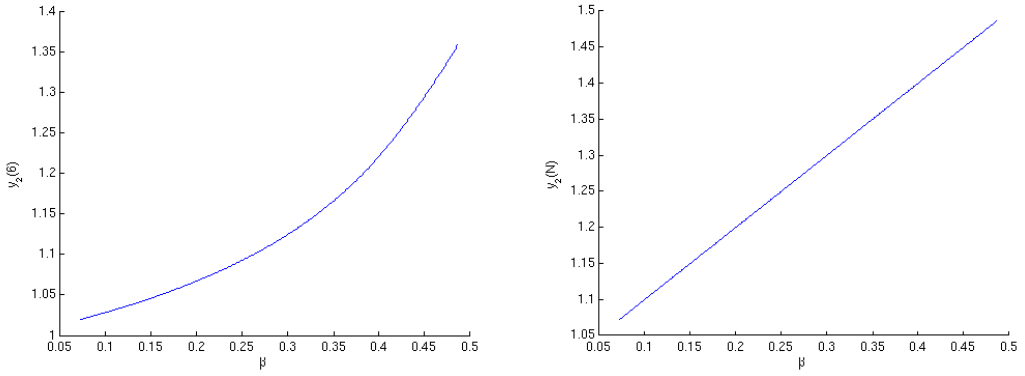

(a) (b)

Figure 6.6: Bifurcation diagram of the dimensionless temperature at (a) the front and (b) the endpoint. β is the active parameter.

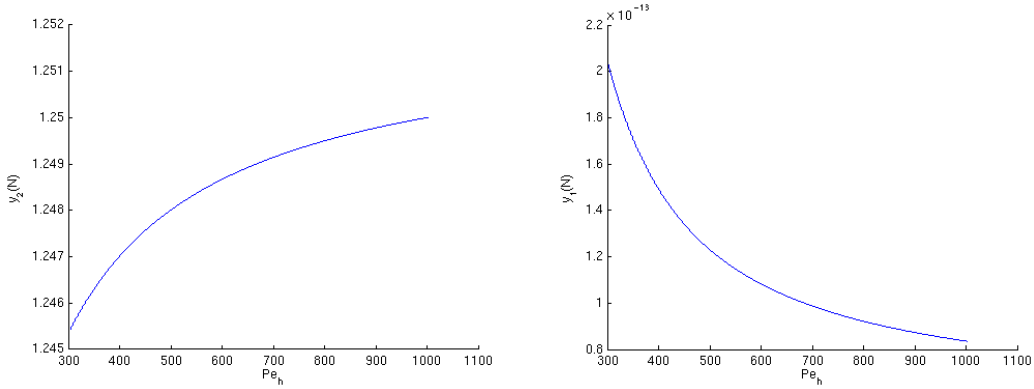

(a) (b)

Figure 6.7: Bifurcation diagram of the dimensionless concentration at (a) the front and (b) the endpoint. Pe_h is the active parameter.

the temperature profiles more even.

6.3.5 The Peclet Number for Mass, Pe_m

The final parameter is Pe_m and the bifurcation diagrams can be seen in figure 6.9 and 6.10. Both these figures confirm the behaviour seen in figure 5.10. No bifurcations were found here either.

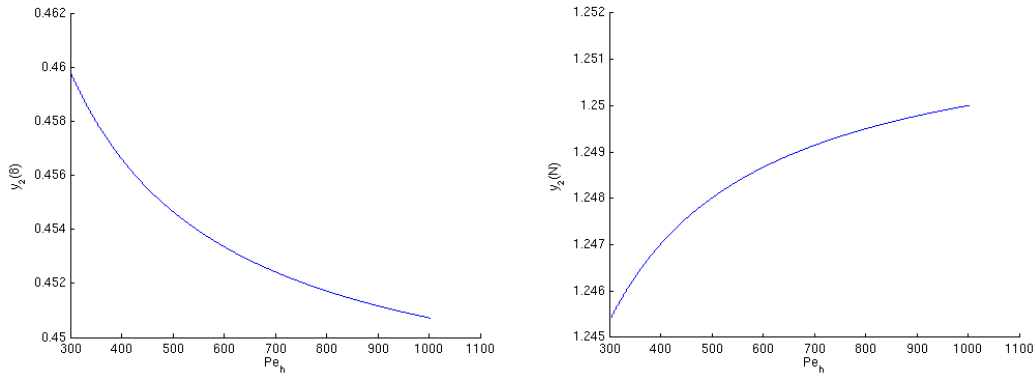

(a) (b)

Figure 6.8: Bifurcation diagram of the dimensionless temperature at (a) the front and (b) the endpoint. Pe_h is the active parameter.

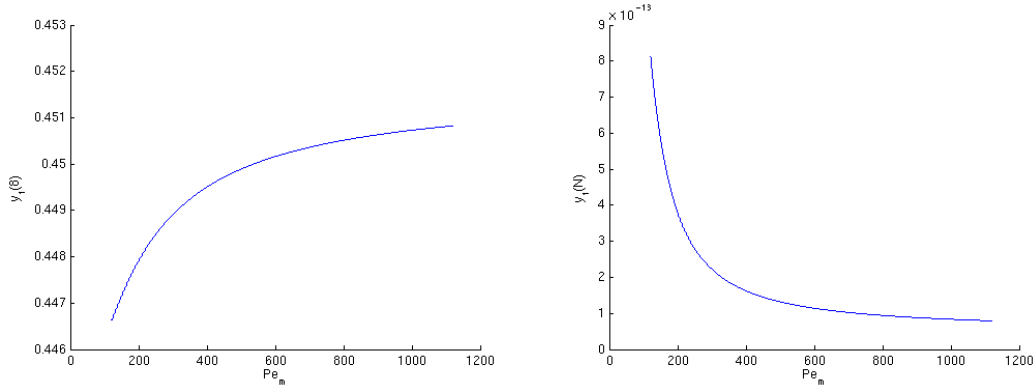

(a) (b)

Figure 6.9: Bifurcation diagram of the dimensionless concentration at (a) the front and (b) the endpoint. Pe_m is the active parameter.

6.3.6 Summary of Results

The bifurcation analysis of the packed-bed reactor model showed that no bifurcations occur in the given parameter space. In [5], some bifurcations are found using this model but these are all consequences of parameter values lying outside the given parameter space. Most of the bifurcations are found for very low values of the Peclet numbers, i.e. $Pe_m = Pe_h < 5$. Such low values actually make the system act like a continuous-stirred tank reactor, which

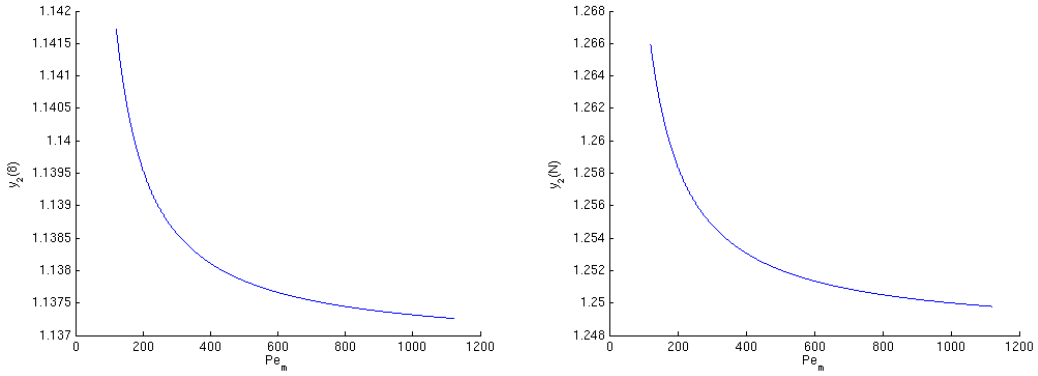

(a) (b)

Figure 6.10: Bifurcation diagram of the dimensionless temperature at (a) the front and (b) the endpoint. Pe_m is the active parameter.

is usually modelled as having no spatial variations in concentration and temperature, see [1]. This is not interesting for this project as industrial packed-bed reactors usually operate with Peclet numbers around 10^3. If any bifurcations actually would have occurred with parameter values inside the given space, they would probably also have been included in [5].
Bifurcation diagrams with heat transfer between the reactor wall and the reaction mixture were also done but they showed no bifurcations either so they are therefore not included.

Chapter 7

The Heat Exchanger Model

The model that has been analysed so far has only described a packed-bed reactor. In this chapter, this model will be extended with a model of a heat exchanger. This new model will then be simulated to see how the steady state looks and how the system reacts when it is subject to process disturbances. First, it will be described what a heat exchanger actually is.

7.1 Theory

A heat exchanger is a device that is used to transfer heat from one substance to another without mixing the two substances. The flow arrangements of heat exchangers can be different from one exchanger to another. A co-current shell and tube heat exchanger consists of a bunch of tubes that are placed inside a shell. The two substances then enter at the same side, one through the tubes and one through the shell over the tubes. They then travel to the other side while exchanging heat on the way, see figure 7.1.

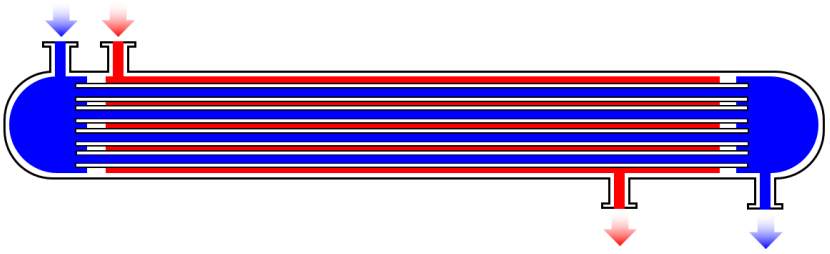

Figure 7.1: A co-current shell and tube heat exchanger.

By using the gas from the outlet of the reactor as the hot substance and the inlet gas to the

system as the cold, the inlet gas can be heated up to an appropriate level before entering the reactor.

How the temperatures of the substances change in the heat exchanger can be seen in figure 7.2. T_3 is the inlet temperature to the heat exchanger, i.e. the outlet temperature of the reactor and T_0 is the inlet temperature to the heat exchanger. ΔT_{app} is the difference between the inlet

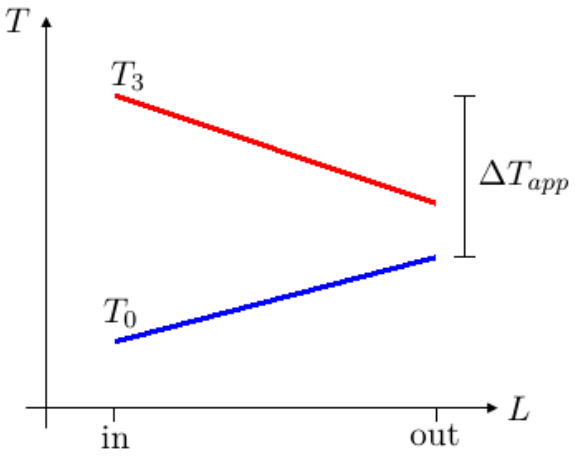

Figure 7.2: Development of the temperatures of the gases as a function of length of the heat exchanger.

temperature of the warm gas and the outlet temperature of the cold gas. This temperature difference is called the temperature approach and the value will typically be between 10 °C and 30 °C. By assuming a constant temperature approach, the outlet temperature of the heat exchanger is

$$T_1 = T_3 - \Delta T_{app}. \tag{7.1}$$

It is not all of the gas with temperature T_0 that should enter the heat exchanger. To be able to control the temperature of the inlet gas to the reactor, a fraction of the gas, α, should actually not go into the heat exchanger. α is usually called the flow fraction and can be adjusted during the process. This means that only a fraction, $(1 - \alpha)$, of the gas enters the heat exchanger. After getting heated up in the heat exchanger, this amount of gas is mixed with the fraction that by-passed the heat exchanger before entering the reactor. This means that the temperature of the inlet gas to the reactor will be

$$T_2 = \alpha T_0 + (1 - \alpha)\, T_1. \tag{7.2}$$

To get a picture of the complete set-up, see figure 7.3. F_0 denotes the gas that enters the system and F_1 is the gas leaving the reactor.

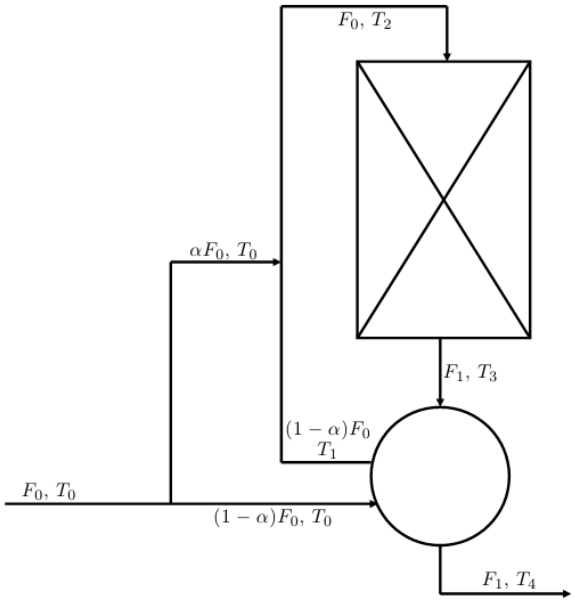

Figure 7.3: The complete set-up. The rectangle represents the packed-bed reactor and the circle represents the heat exchanger.

7.2 Dimensionless Variables

To make the equations congruent with the model for the packed-bed reactor, they have to be turned into dimensionless form. As in chapter 2, this is done relative to T_0. This means that the dimensionless inlet temperature to the system is

$$\lambda_0 = \frac{T_0}{T_0}, \tag{7.3}$$

the dimensionless outlet temperature of the heat exchanger is

$$\lambda_1 = \frac{T_1}{T_0}, \tag{7.4}$$

the dimensionless temperature of the inlet gas to the reactor is

$$\lambda_2 = \frac{T_2}{T_0}, \tag{7.5}$$

while the dimensionless temperature of the outlet gas from the reactor is

$$\lambda_3 = \frac{T_3}{T_0}. \tag{7.6}$$

Finally the dimensionless temperature approach is

$$\Delta\lambda_{app} = \frac{\Delta T_{app}}{T_0}. \tag{7.7}$$

Solving for T_1, T_3 and ΔT_{app} in (7.4), (7.6) and (7.7) and inserting the found expressions into (7.1) yield

$$\lambda_1 T_0 = \lambda_3 T_0 - \Delta\lambda_{app} T_0 \quad \Leftrightarrow \tag{7.8}$$

$$\lambda_1 = \lambda_3 - \Delta\lambda_{app}. \tag{7.9}$$

In the same way it can be found that

$$\lambda_2 T_0 = \alpha T_0 + (1-\alpha)\lambda_1 T_0 \quad \Leftrightarrow \tag{7.10}$$

$$\lambda_2 = \alpha\lambda_0 + (1-\alpha)\lambda_1. \tag{7.11}$$

This means that the complete model for the temperatures in the heat exchanger is

$$\lambda_1 = \lambda_3 - \Delta\lambda_{app}, \tag{7.12}$$

$$\lambda_2 = \alpha\lambda_0 + (1-\alpha)\lambda_1. \tag{7.13}$$

Together with (2.25)-(2.31), these equations then constitute the complete model.

7.3 Steady State of the Complete Model

The MatLab implementation of the complete model can be found in appendix A.7. Simulations are now made to see the concentration and temperature development over time and they can be seen in figure 7.4 and 7.5.

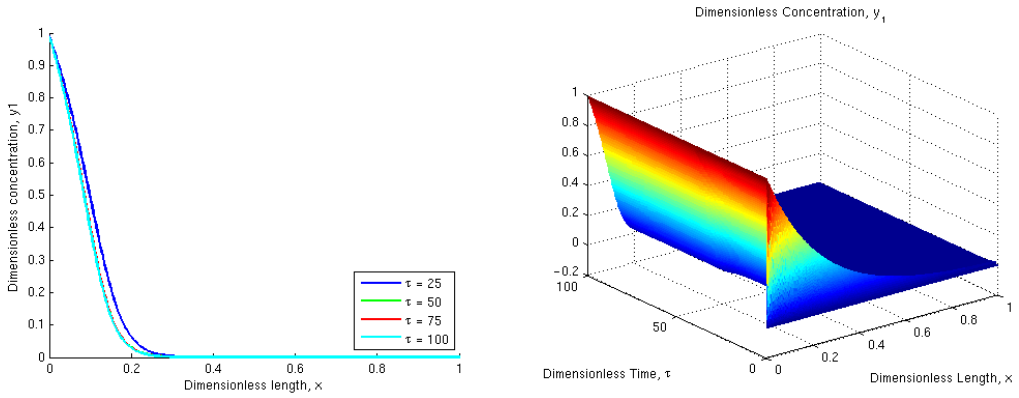

(a) (b)

Figure 7.4: Dimensionless concentration simulations of the complete model. (a) shows dimensionless concentration profiles for different times and (b) shows the development in dimensionless concentration as a function of time and length. The parameters have the values $Pe_m = 1000$, $Pe_h = 1000$, $Le = 40$, $\beta = 0.25$, $Da = 4$, $\gamma = 11$, $H_w = 0.5$, $y_{2w} = 1$, $\alpha = 0.9$, $\Delta\lambda_{app} = 0.1$.

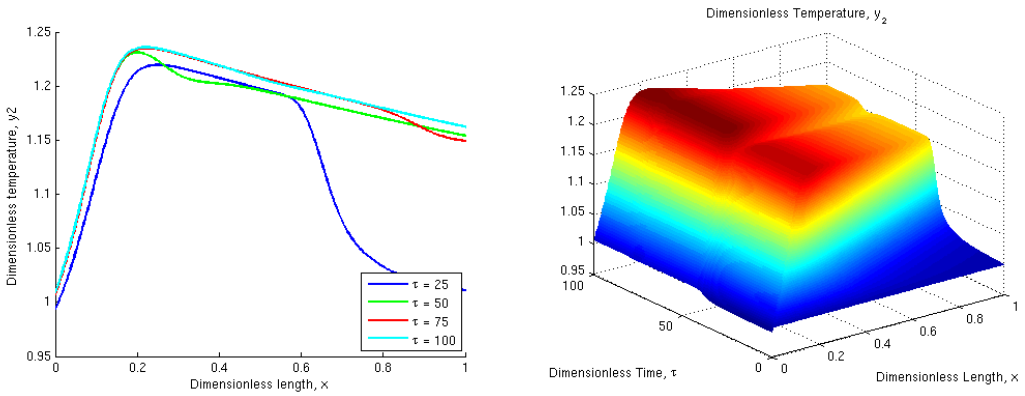

(a) (b)

Figure 7.5: Dimensionless temperature simulations of the complete model. (a) shows dimensionless temperature profiles for different times and (b) shows the development in dimensionless temperature as a function of time and length. The parameters have the values $Pe_m = 1000$, $Pe_h = 1000$, $Le = 40$, $\beta = 0.25$, $Da = 4$, $\gamma = 11$, $H_w = 0.5$, $y_{2w} = 1$, $\alpha = 0.9$, $\Delta\lambda_{app} = 0.1$.

7.4 Parameter Effects

Like it was done in chapter 5.2, it will now be investigated how the steady state is affected by changes in the new parameters α and $\Delta\lambda_{app}$. $H_w = 0.5$ and $y_{2w} = 1$ while the rest of the parameters have the values given by (5.1).

7.4.1 The Flow Factor, α

The flow fraction, α, is defined as the fraction of the flow that is by-passing the heat exchanger. Therefore the temperature of the reaction mixture in the reactor should grow as the flow factor decreases because more of the inlet flow is heated up this way. This behaviour can be confirmed by figure 7.6, which shows the steady state of the system for different values of α.

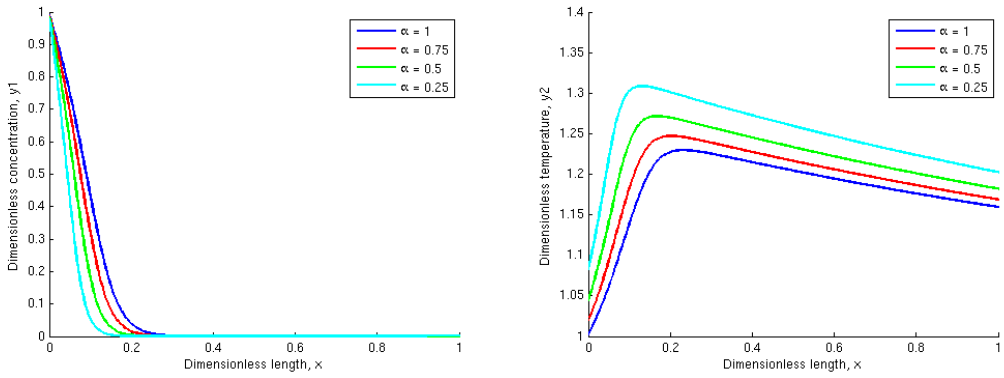

(a) The dimensionless concentration.

(b) The dimensionless temperature.

Figure 7.6: Dimensionless concentration and dimensionless temperature profiles of the steady state for varying values of α.

7.4.2 The Dimensionless Temperature Approach, $\Delta\lambda_{app}$

The steady state of the system for different values of $\Delta\lambda_{app}$ can be seen in figure 7.7. As $\Delta\lambda_{app}$ increases, the temperature of the reaction mixture falls. This is because large values of $\Delta\lambda_{app}$ yield lower values of λ_1 and therefore lower values of the inlet temperature to the reactor.

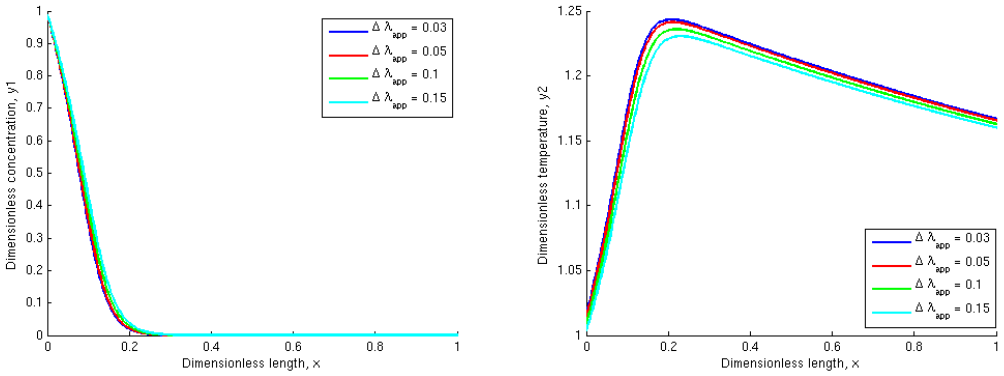

(a) The dimensionless concentration.

(b) The dimensionless temperature.

Figure 7.7: Dimensionless concentration and dimensionless temperature profiles of the steady state for varying values of $\Delta\lambda_{app}$.

7.5 Convective Instability and the Snowball Effect

To investigate the convective instability of the system with an integrated heat exchanger, the same approach as in section 5.1 is taken. This means that the steady state is found and the value of λ_0 is changed from 1 to 0.95 after some time, i.e. a step disturbance of -5% is added to the dimensionless inlet temperature of the system. The model is then simulated for more time. A plot of the temperature as a function of time and length of the reactor can be seen in figure 7.8. Due to the convective instability and wrong-way behaviour of the packed-bed reactor, the negative disturbance to the inlet temperature is amplified as described in section 5.1. Because of the heat exchanger, this amplified disturbance is fed back to the reactor where it is amplified again and so on. This causes a snowball effect illustrated by growing oscillations in temperature. These oscillations do not continue to grow though. In figure 7.9, the simulation has been run for even longer time, i.e. until $\tau = 200$. Here it can be seen that the outlet temperature actually reaches a maximum value of around $y_{2out} = 1.75$ and that the temperature of the whole distribution reaches a maximum value of around $y_{2max} = 1.8$. It is hard to tell if the solution is periodic or approaches a new steady state from this figure though. Figure 7.10, on the other hand, shows the temperature in the middle of the reactor as a function of time together with the phase portrait for the middle of the reactor. Figure 7.10a shows that the solution is still oscillating even for $\tau = 200$ and figure 7.10b shows

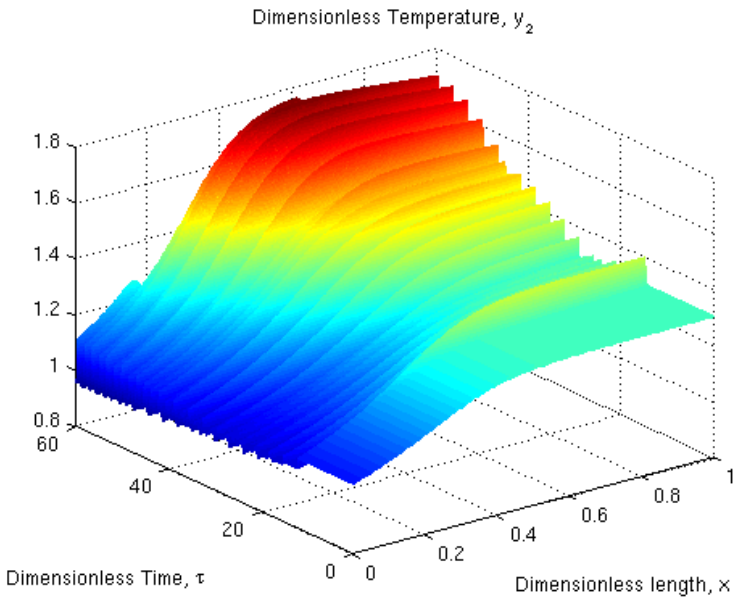

Figure 7.8: The dimensionless temperature as a function of length and time for the system with an integrated heat exchanger. The parameter values are $Pe_m = 1000$, $Pe_h = 1000$, $Le = 3$, $\beta = 0.25$, $Da = 1$, $\gamma = 11$, $\alpha = 0.75$, $\Delta\lambda_{app} = 0.1$.

that the solution approaches a limit cycle. This means that a periodic solution has actually been found. This will be discussed further in the following chapter. Including the terms describing heat transfer between the reaction mixture and the reactor wall also has a big influence on the snowball effect. The temperature distribution then looks like figure 7.11. After the disturbance has been applied, a moving hot spot occurs but instead of giving rise to oscillations with growing amplitude, the oscillations have decaying amplitudes until they are washed out. This means that a cold reactor wall can neutralize the snowball effect.

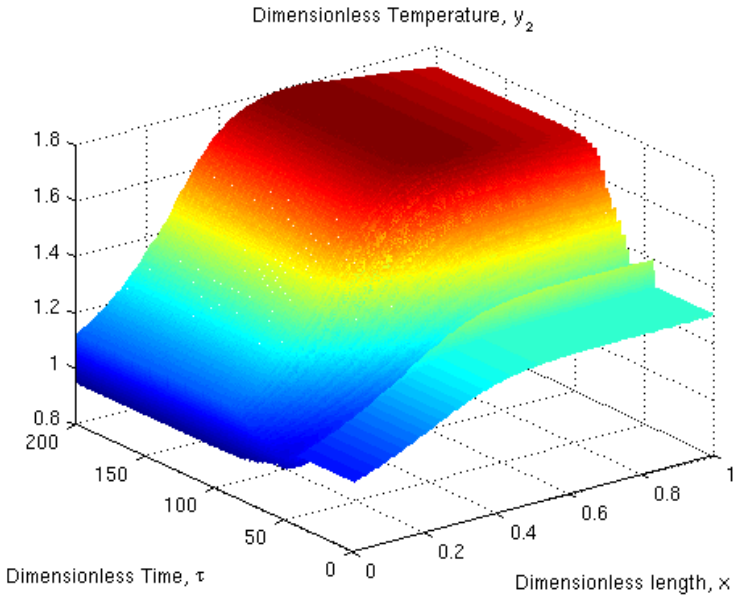

Figure 7.9: The dimensionless temperature as a function of length and time for the system with an integrated heat exchanger. The simulation is run until $\tau = 200$. The parameter values are $Pe_m = 1000$, $Pe_h = 1000$, $Le = 3$, $\beta = 0.25$, $Da = 1$, $\gamma = 11$, $\alpha = 0.75$, $\Delta\lambda_{app} = 0.1$.

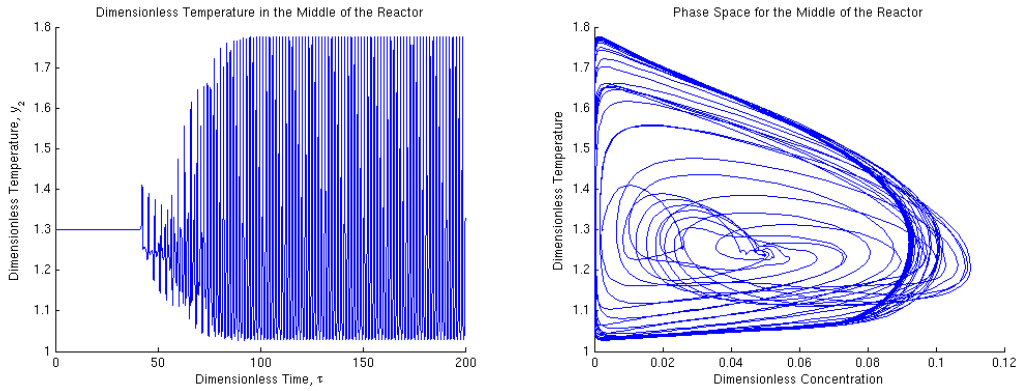

(a) (b)

Figure 7.10: (a) shows the dimensionless temperature in the middle of the reactor as a function of time and (b) shows the phase portrait for the middle of the reactor.

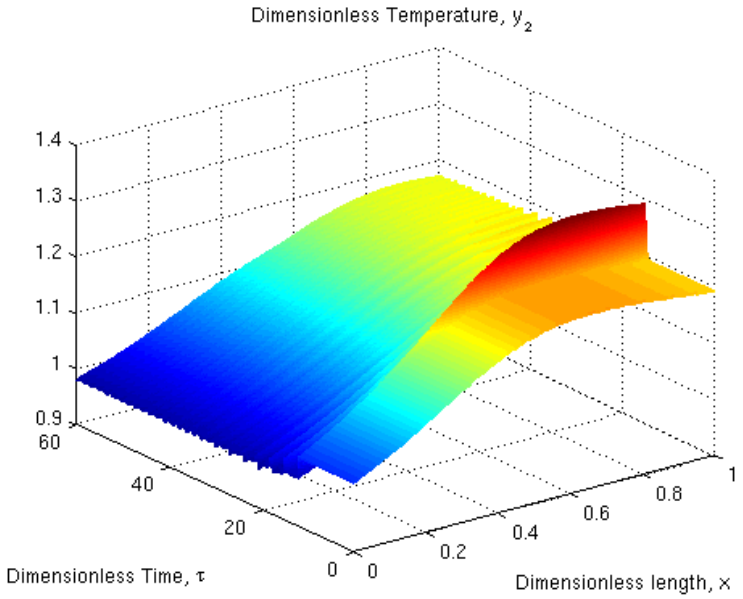

Figure 7.11: The dimensionless temperature as a function of length and time for the system with an integrated heat exchanger and heat transfer to the reactor wall. The parameter values are $Pe_m = 1000$, $Pe_h = 1000$, $Le = 3$, $\beta = 0.25$, $Da = 1$, $\gamma = 11$, $\alpha = 0.75$, $\Delta\lambda_{app} = 0.1$, $H_w = 0.5$, $y_{2w} = 1$.

Chapter 8

Bifurcation Analysis of the Complete Model

In this chapter, bifurcation analysis will be performed on the complete system model, i.e. the model of the packed-bed reactor combined with the model of the heat exchanger. Initially this will be done under the assumption that there is no heat transfer between the reactor wall and the reaction mixture. In the last part of the chapter, bifurcation analysis will be done on the system when this assumption is not used. The results will then be compared.
Just like in chapter 6, the parameters that are not analysed will have the values (5.1).
Not all of the parameters will be subjects to bifurcation analysis as it was previously shown that they did not affect the steady state much. The focus will be on Da, β and the newly introduced parameters α and $\Delta\lambda_{app}$. Analysis of the other parameters will also be done but the diagrams will not be presented. The values of any bifurcation points that might occur for the other parameters will be presented in section 8.3.

8.1 Model without Heat Transfer to the Reactor Wall

At first it will be assumed that there is no heat transfer between the reactor wall and the reaction mixture. The analysis will start with Da.

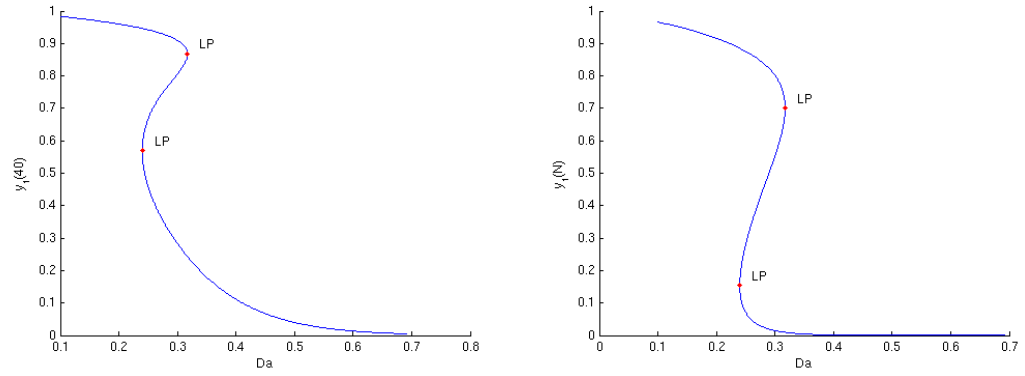

(a) (b)

Figure 8.1: Bifurcation diagram of the dimensionless concentration at (a) the middle of the reactor and (b) the endpoint. Da is the active parameter, $\Delta\lambda_{app} = 0.1$ and $\alpha = 0.5$.

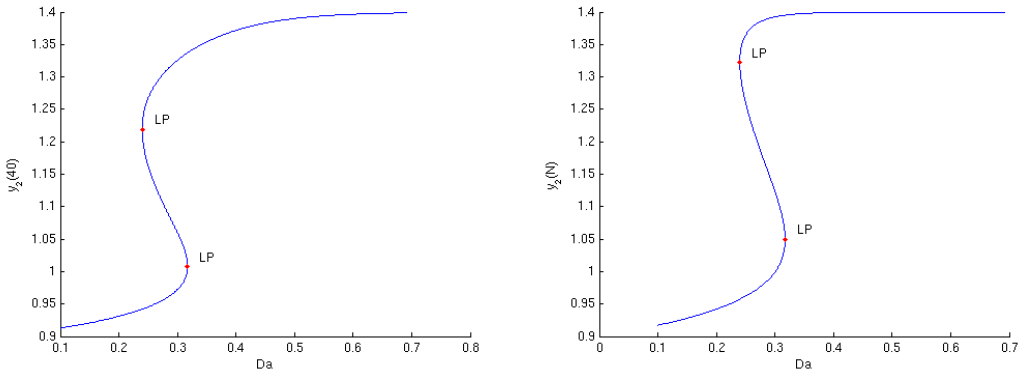

(a) (b)

Figure 8.2: Bifurcation diagram of the dimensionless temperature at (a) the middle of the reactor and (b) the endpoint. Da is the active parameter, $\Delta\lambda_{app} = 0.1$ and $\alpha = 0.5$.

8.1.1 The Damköhler Number, Da

To do this analysis, $\Delta\lambda_{app}$ is set to 0.1, while α will be varied so that one can see both the effect of changes in Da and in α. At first, α will have the value 0.5. The bifurcation diagram for the concentration and the temperature can be seen in figure 8.1 and 8.2 respectively. Note that the figures show diagrams for both the middle of the reactor and the outlet. Furthermore, the figures only show the bifurcation diagrams for values of Da below ~ 0.7. This is because

nothing interesting happens for higher values of Da. Here, two limit point bifurcations have arisen at $Da_1 = 0.24$ and $Da_2 = 0.32$. This means that three different steady states coexist between Da_1 and Da_2. Examination of the eigenvalues show that they all have negative real part before the bifurcation point Da_2 and that one real eigenvalue is zero at the bifurcation point. This means that the steady states between the two bifurcation points are unstable, while the bigger branches are stable.

Suppose now that the system starts in the stable steady state with $Da = 0.1$. Da is then slowly increased until it reaches the bifurcation point Da_2. The system then jumps to the steady state on the other stable branch, hence avoiding the unstable area. Increasing Da will just make the system follow the new stable branch but if one wants to return to the original stable branch, Da has to be decreased slowly to the value of Da_1, where the system then jumps back to the original stable branch. This phenomenon is called hysteresis.

Furthermore, it turns out that a complex conjugate pair of eigenvalues has zero real part at the point $Da_3 = 0.4$. A plot of the eigenvalues for a value of $Da = 0.39$ and a value of $Da = 0.4$ can be seen in figure 8.3. Zooming in on the critical eigenvalues, i.e. the eigenvalues with real part closest to zero, yield the plot from figure 8.4. This shows that a complex pair of eigenvalues actually has zero real part for $Da = 0.4$. According to section 6.1, a Hopf bifurcation has actually occurred, which was not detected by MatCont. The eigenvalues will therefore be analysed in this way in the rest of this report to make sure that all bifurcations are found.

To summarize, the lower branches in figure 8.1 and 8.2 are stable, the steady states between Da_2 and Da_1 are unstable and the high branch is stable between Da_1 and Da_3, where a Hopf bifurcation occurs.

The analysis of Da is also done with a value of the flow factor of $\alpha = 0.25$. The bifurcation diagrams can be seen in figure 8.5 and 8.6. Here, limit point bifurcations occur at $Da_1 = 0.06$ and $Da_2 = 2.34$. Like before, by checking the eigenvalues, it can be seen that there is an area of unstable steady states between these two values of Da. For $\alpha = 0.5$ this area is quite small but because of the lower value of α, more heat is entering the reactor and it can be concluded that this heat is expanding the area of unstable steady states.

By comparing figure 8.6b and 8.2b it can also be concluded that the outlet temperature gets higher for lower values of α.

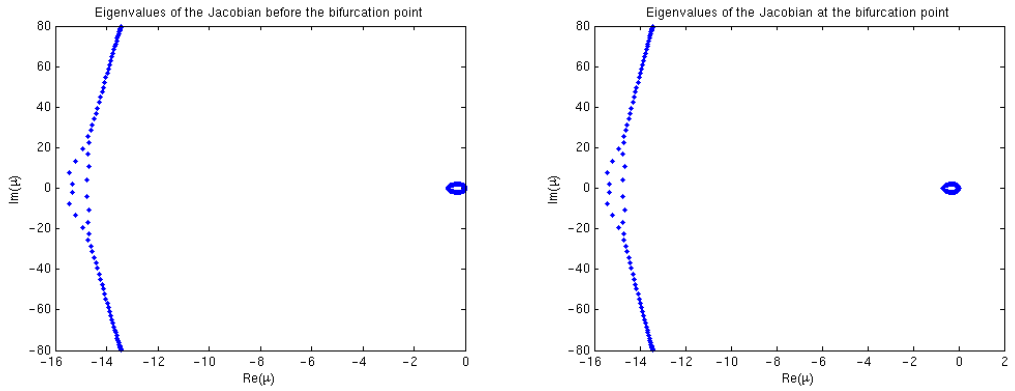

(a) (b)

Figure 8.3: (a) The eigenvalues right before the bifurcation point, Da_3, and (b) at the bifurcation point, Da_3.

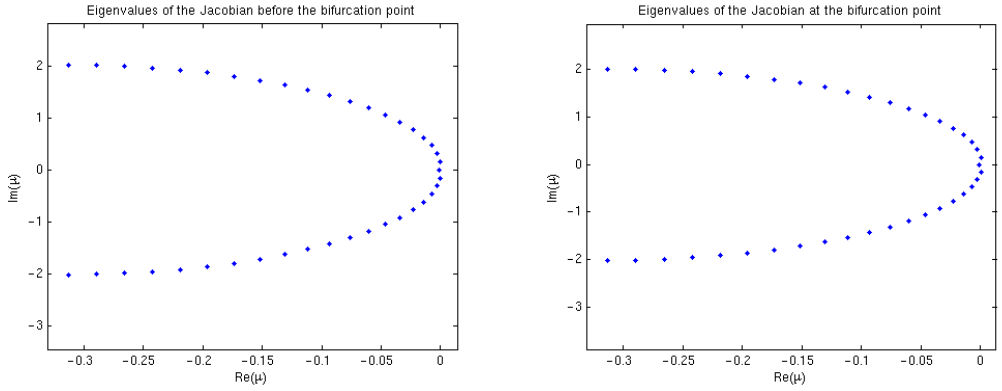

(a) (b)

Figure 8.4: (a) Zoom of the eigenvalues right before the bifurcation point, Da_3, and (b) at the bifurcation point, Da_3.

Finally bifurcation analysis for Da is also done with the parameter values

$$Pe_m = 1000,\ Pe_h = 1000,\ Le = 3,\ \beta = 0.25,\ \gamma = 11,\ \alpha = 0.75,\ \Delta\lambda_{app} = 0.1,$$

which are the same as the ones used in figure 7.8. The bifurcation diagram for the outlet temperature can be seen in figure 8.7. This diagram shows no bifurcations but a complex conjugate pair of eigenvalues actually lie on the imaginary axis when $Da = 0.4$, meaning that

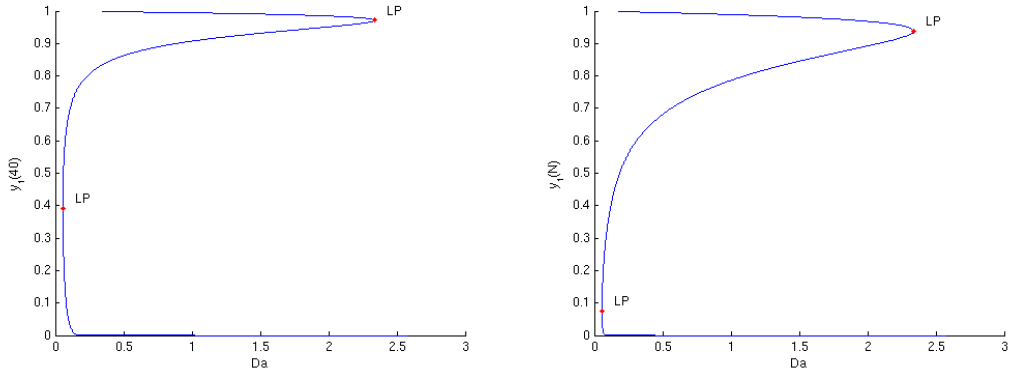

(a) (b)

Figure 8.5: Bifurcation diagram of the dimensionless concentration at (a) the middle of the reactor and (b) the endpoint. Da is the active parameter, $\Delta\lambda_{app} = 0.1$ and $\alpha = 0.25$.

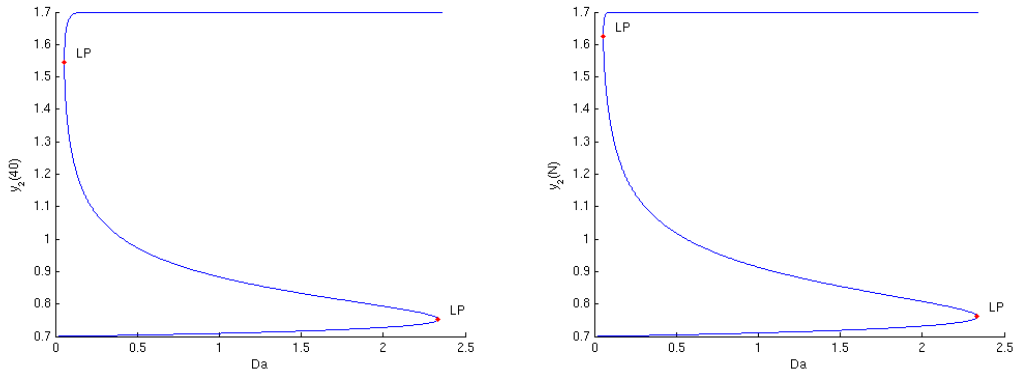

(a) (b)

Figure 8.6: Bifurcation diagram of the dimensionless temperature at (a) the middle of the reactor and (b) the endpoint. Da is the active parameter, $\Delta\lambda_{app} = 0.1$ and $\alpha = 0.25$.

a Hopf bifurcation takes place for this value, see figure 8.8. By examining figure 7.10b it seems that this Hopf bifurcation is supercritical. This means that for $Da = 1$, the solution should turn periodic when a disturbance is added to the system and this is exactly what happens in figure 7.8. On the other hand, when $Da < 0.4$, the system is stable and a disturbance will

therefore just be washed out.

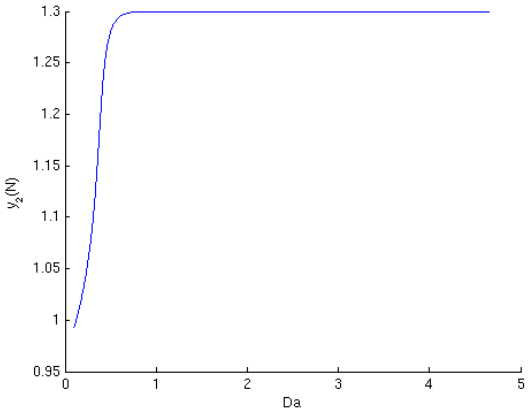

Figure 8.7: The bifurcation diagram of the dimensionless outlet temperature. Da is the active parameter. The other parameters have the values $Pe_m = 1000$, $Pe_h = 1000$, $Le = 3$, $\beta = 0.25$, $\gamma = 11$, $\alpha = 0.75$, $\Delta\lambda_{app} = 0.1$.

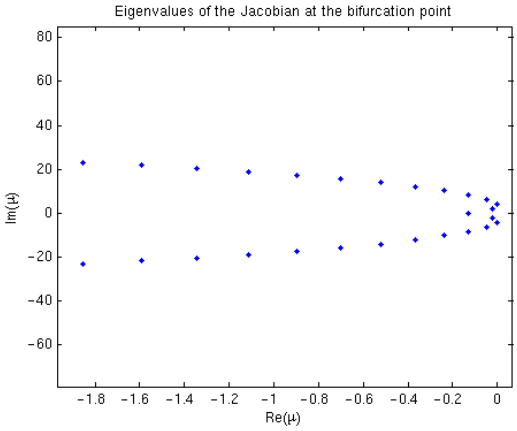

Figure 8.8: The eigenvalues for $Da = 0.4$. The other parameters have the values $Pe_m = 1000$, $Pe_h = 1000$, $Le = 3$, $\beta = 0.25$, $\gamma = 11$, $\alpha = 0.75$, $\Delta\lambda_{app} = 0.1$.

8.1.2 The Dimensionless Temperature Approach, $\Delta\lambda_{app}$

The next parameter is the dimensionless temperature approach. Setting $\alpha = 0.5$ gives rise to the bifurcation diagrams seen in figure 8.9 and 8.10. Here limit point bifurcations are found

at $\Delta\lambda_{app1} = 0.28$ and $\Delta\lambda_{app2} = 0.40$. Examination of the eigenvalues show that the steady states between the two bifurcation points are unstable and that the two other branches are stable. Furthermore the analysis of the eigenvalues show that a Hopf bifurcation occurs at $\Delta\lambda_{app} = 0.13$. The eigenvalues will not be shown here though.

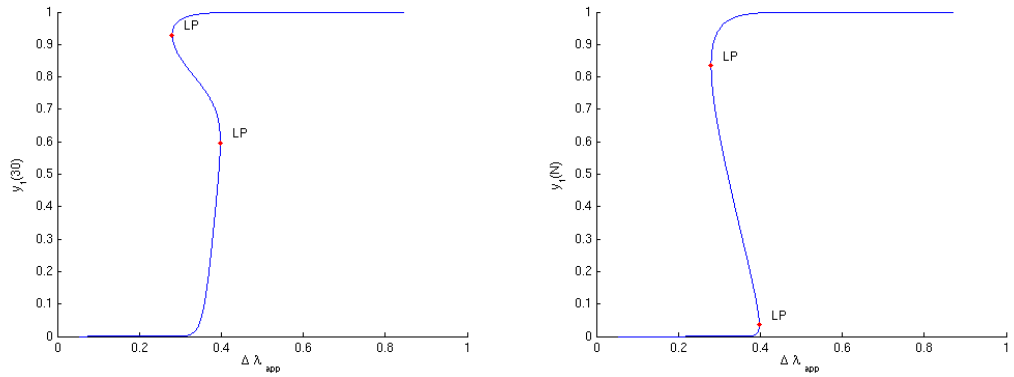

(a) (b)

Figure 8.9: Bifurcation diagram of the dimensionless concentration at (a) the middle of the reactor and (b) the endpoint. $\Delta\lambda_{app}$ is the active parameter and $\alpha = 0.5$.

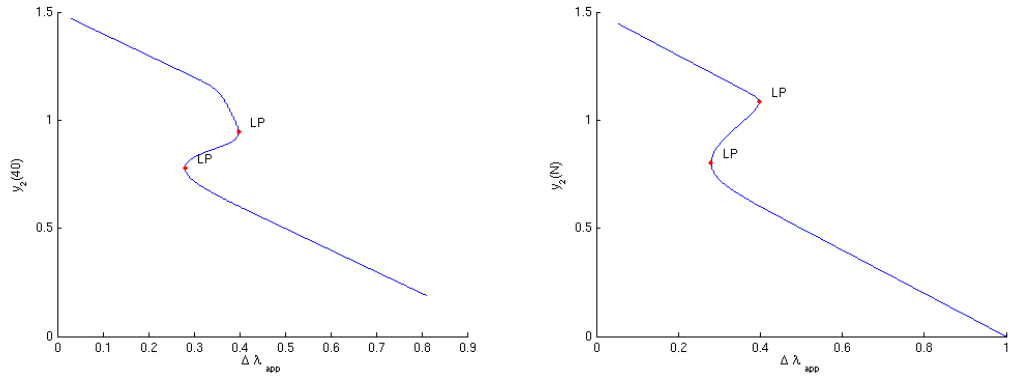

(a) (b)

Figure 8.10: Bifurcation diagram of the dimensionless temperature at (a) the middle of the reactor and (b) the endpoint. $\Delta\lambda_{app}$ is the active parameter and $\alpha = 0.5$.

Like in the previous section bifurcation analysis was also done for $\alpha = 0.25$. The diagrams will not be shown here as they are very similar to the diagrams for $\alpha = 0.5$. The difference

is that the area of unstable steady states becomes larger for $\alpha = 0.25$. In fact this is the case for all the parameters. The area of unstable steady states becomes larger for smaller values of α. The analysis of the different parameters will therefore only be done for $\alpha = 0.5$ in the following.

8.1.3 The Flow Factor, α

To do the analysis of the flow factor, the dimensionless temperature approach is set to $\Delta\lambda_{app} = 0.1$. The bifurcation diagrams can be seen in figure 8.11 and 8.12. They show no bifurcations but a Hopf bifurcation actually occurs here at $\alpha = 0.55$. The steady state is stable for $\alpha > 0.55$ and unstable for $\alpha \leq 0.55$. These results fit with the fact that less heat is transferred back to the reactor when α increases.

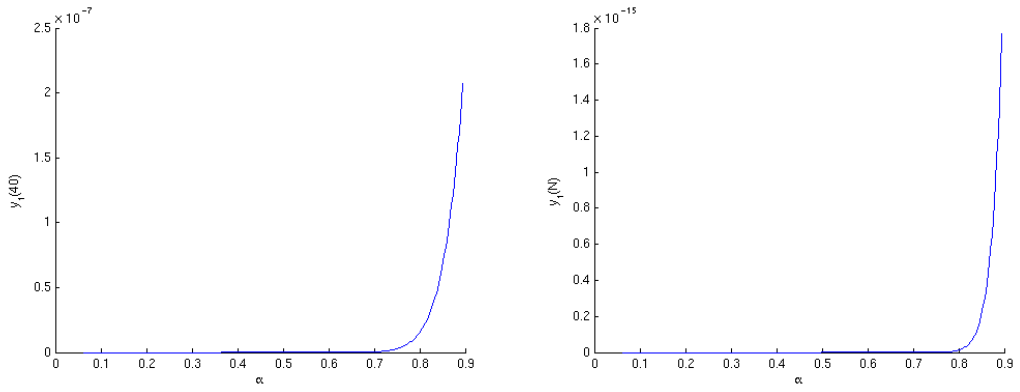

(a) (b)

Figure 8.11: Bifurcation diagram of the dimensionless concentration at (a) the middle of the reactor and (b) the endpoint. α is the active parameter and $\Delta\lambda_{app} = 0.1$.

8.1.4 The Dimensionless Adiabatic Temperature Rise, β

Finally, bifurcation analysis will be done for β. For $\alpha = 0.5$ and $\Delta\lambda_{app} = 0.1$, the bifurcation diagrams can be seen in figure 8.13 and 8.14. Even though the diagrams show no bifurcations, the eigenvalues reveal that a Hopf bifurcation takes place at $\beta = 0.18$. The steady state is stable for $\beta < 0.18$ and unstable for $\beta \geq 0.18$.

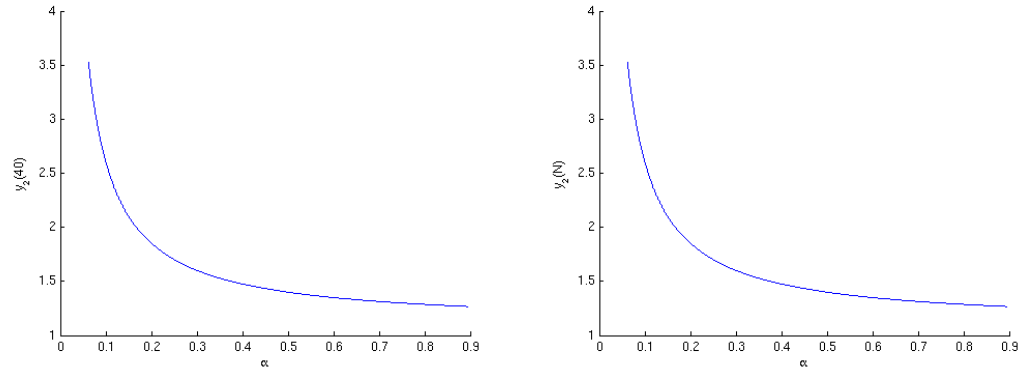

(a) (b)

Figure 8.12: Bifurcation diagram of the dimensionless temperature at (a) the middle of the reactor and (b) the endpoint. α is the active parameter and $\Delta\lambda_{app} = 0.1$.

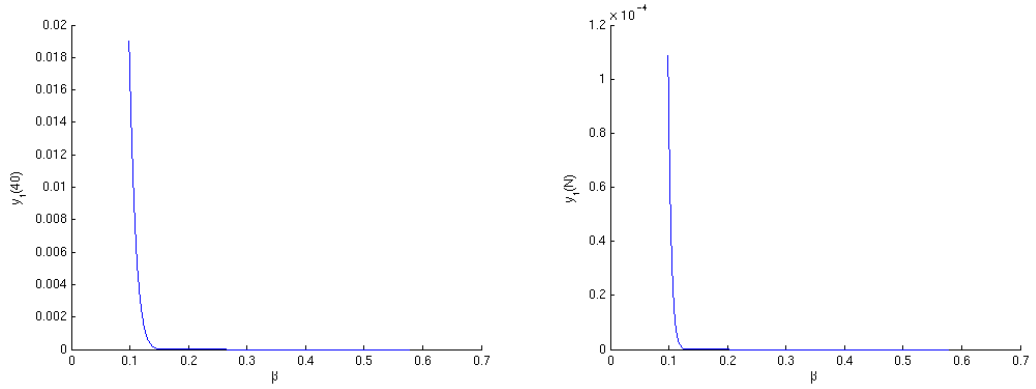

(a) (b)

Figure 8.13: Bifurcation diagram of the dimensionless concentration at (a) the middle of the reactor and (b) the endpoint. β is the active parameter and $\alpha = 0.5$.

8.2 Model with Heat Transfer to the Reactor Wall

In this section it will be assumed that there is heat transfer between the reactor wall and the reaction mixture and then bifurcation analysis will be performed for the parameters Da, $\Delta\lambda_{app}$ and α. The dimensionless wall temperature is set to $y_{2w} = 1$ and the dimensionless heat transfer coefficient is set to $H_w = 0.5$ for the rest of this section.

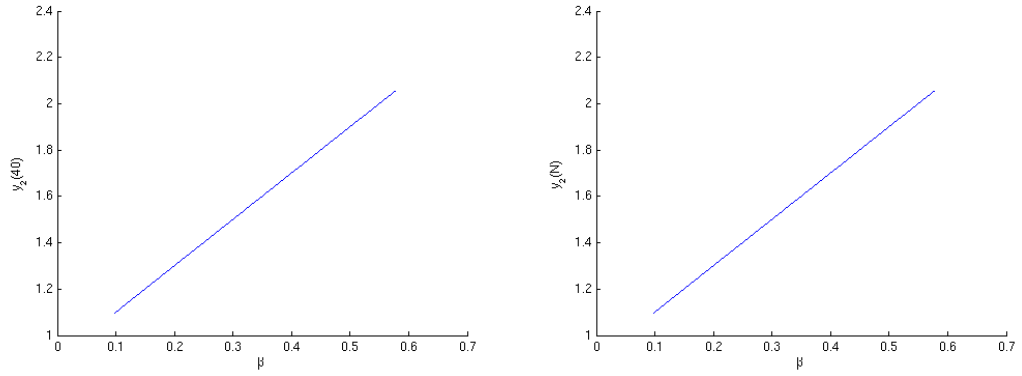

(a) (b)

Figure 8.14: Bifurcation diagram of the dimensionless temperature at (a) the middle of the reactor and (b) the endpoint. β is the active parameter and $\alpha = 0.5$.

8.2.1 The Damköhler Number, Da

The bifurcation diagrams for the Damköhler number can be seen in figure 8.15 and 8.16. As opposed to when heat transfer to the reactor wall was not assumed these diagrams show no limit point bifurcations. There is although a Hopf bifurcation at $Da = 0.4$.

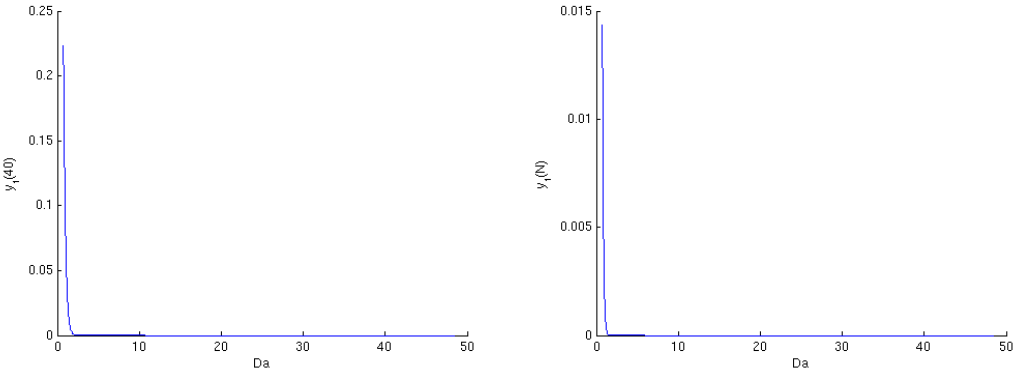

(a) (b)

Figure 8.15: Bifurcation diagram of the dimensionless concentration at (a) the middle of the reactor and (b) the endpoint. Da is the active parameter and $\alpha = 0.5$. Heat transfer between the reaction mixture and the reactor wall is assumed here.

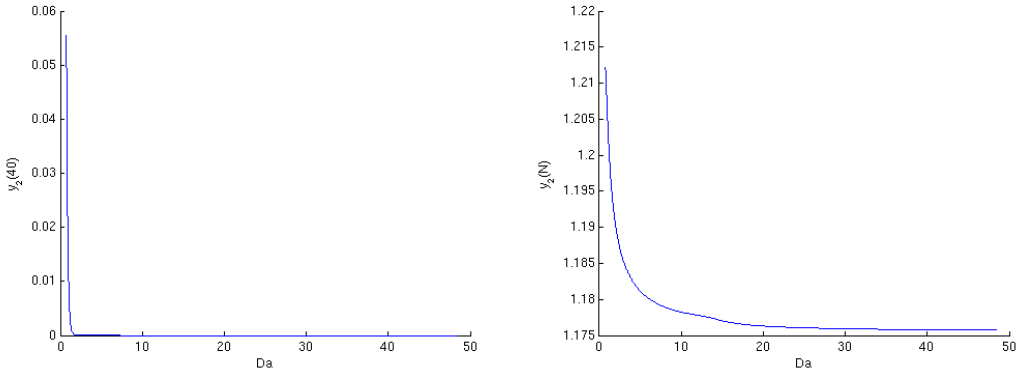

(a) (b)

Figure 8.16: Bifurcation diagram of the dimensionless temperature at (a) the middle of the reactor and (b) the endpoint. Da is the active parameter and $\alpha = 0.5$. Heat transfer between the reaction mixture and the reactor wall is assumed here.

8.2.2 The Dimensionless Temperature Approach, $\Delta\lambda_{app}$

The value of α is set to 0.5 and the bifurcation diagrams can be seen in figure 8.17 and 8.18. Limit point bifurcations occur at $\Delta\lambda_{app1} = 0.44$ and $\Delta\lambda_{app2} = 0.46$. When comparing these

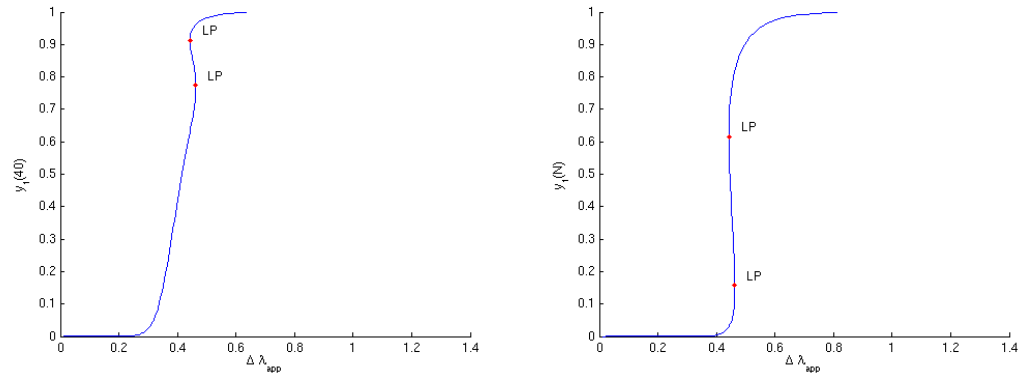

(a) (b)

Figure 8.17: Bifurcation diagram of the dimensionless concentration at (a) the middle of the reactor and (b) the endpoint. $\Delta\lambda_{app}$ is the active parameter and $\alpha = 0.5$. Heat transfer between the reaction mixture and the reactor wall is assumed here.

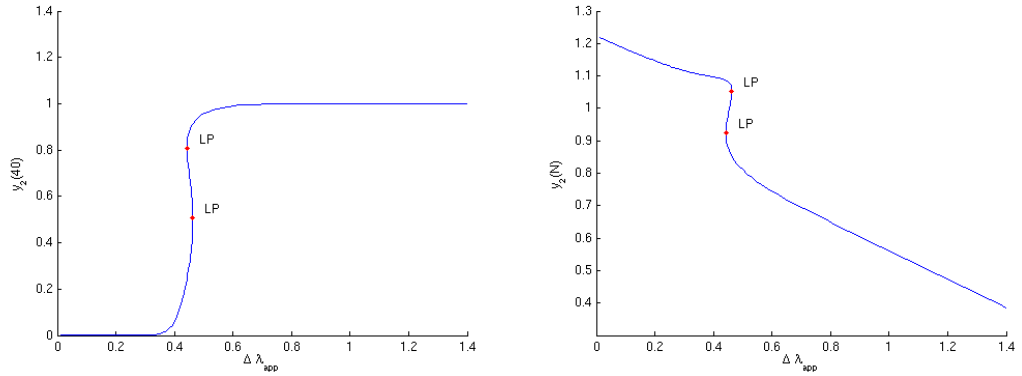

(a) (b)

Figure 8.18: Bifurcation diagram of the dimensionless temperature at (a) the middle of the reactor and (b) the endpoint. $\Delta\lambda_{app}$ is the active parameter and $\alpha = 0.5$. Heat transfer between the reaction mixture and the reactor wall is assumed here.

figures to figure 8.9 and 8.10 it is clear that the unstable region becomes smaller when heat transfer is assumed. Furthermore there are no Hopf bifurcations here.

8.2.3 The Flow Factor, α

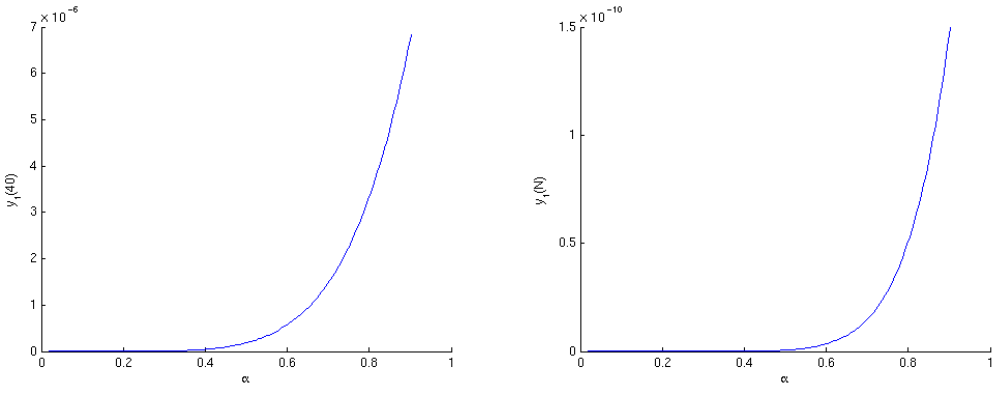

(a) (b)

Figure 8.19: Bifurcation diagram of the dimensionless concentration at (a) the middle of the reactor and (b) the endpoint. α is the active parameter and $\Delta\lambda_{app} = 0.1$. Heat transfer between the reaction mixture and the reactor wall is assumed here.

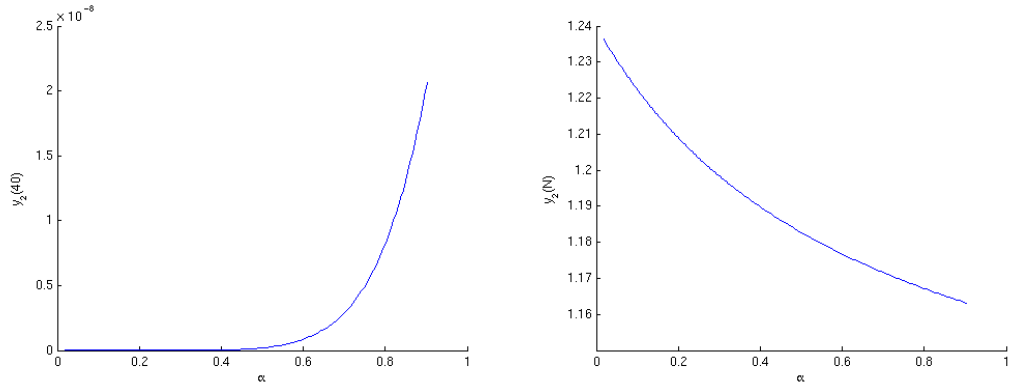

(a) (b)

Figure 8.20: Bifurcation diagram of the dimensionless temperature at (a) the middle of the reactor and (b) the endpoint. α is the active parameter and $\Delta\lambda_{app} = 0.1$. Heat transfer between the reaction mixture and the reactor wall is assumed here.

The bifurcation diagrams with α as the active parameter can be seen in figure 8.19 and 8.20. They show no limit point bifurcations and an examination of the eigenvalues show that there are no Hopf bifurcations as well.

8.3 Summary of Results

Besides the analysis of the parameters that was presented here, bifurcation analysis was also done for the parameters γ, Pe_m and Pe_h. A complete summary of the occurrence of the different bifurcation points can be seen in table 8.1. Note that this table only shows where the bifurcations occur but not which steady states are stable.

This table shows that both limit points bifurcations and Hopf bifurcations occur for the packed-bed reactor model with an integrated heat exchanger. These bifurcations occurred for changes in the parameters Da, β, $\Delta\lambda_{app}$ and α while changing the parameters γ, Pe_m and Pe_h did not yield any bifurcations. The analysis of Da without heat transfer to the reactor wall showed both limit point bifurcations and Hopf bifurcations and when there was heat transfer, there were no longer any limit point bifurcations. The analysis of $\Delta\lambda_{app}$ also showed both kind of bifurcations but when the heat transfer assumption was used, there were no longer any Hopf bifurcations. The analysis of α showed that there are no Hopf bifurcations

	$y_{2w} = y_2$			$y_{2w} \neq y_2$		
Parameter \ Bifurcations	LP_1	LP_2	Hopf	LP_1	LP_2	Hopf
Da	0.24	0.32	0.31	-	-	0.4
β	-	-	0.18	-	-	0.19
γ	-	-	-	-	-	-
Pe_m	-	-	-	-	-	-
Pe_h	-	-	-	-	-	-
$\Delta\lambda_{app}$	0.28	0.40	0.13	0.44	0.46	-
α	-	-	0.55	-	-	-

Table 8.1: Summary of the occurrence of bifurcations for $\alpha = 0.5$ and $\Delta\lambda_{app} = 0.1$. - means that the given bifurcation type does not occur when the parameter is changed.

when heat transfer to the reactor wall is assumed. In general, fewer bifurcations were found when heat transfer is assumed, as the chosen wall temperature of $y_{2w} = 1$ cools down the reactor and makes it less likely for instabilities to occur.

Chapter 9

Discussion

It was shown in this report that there are many problematic areas when operating a packed-bed reactor. Even when a heat exchanger is not integrated with the reactor, convective instability can cause moving hot spots that can deactivate the catalyst and might even pose a safety hazard. These moving hot spots do have a maximum value though and the system will always return to a stable steady state. It was namely shown with bifurcation analysis that no bifurcations will occur when changing any of the 6 parameters in the given parameter space. Because all the steady states are stable it is relatively easy to operate and control the packed-bed reactor.

It is although rarely the case that a packed-bed reactor is not integrated with a heat exchanger to heat up the inlet gas in an efficient way and this makes the situation way more complex. Because of the integration of the heat exchanger, the bifurcation analysis showed existence of both limit point- and Hopf bifurcations. These are very undesirable as they cause hysteresis and large-amplitude oscillations of temperature. The bifurcations occurred for the parameters Da, β, α and $\Delta\lambda_{app}$. The first three of these parameters can usually be controlled by the operator of the system so it is actually possible for the operator to avoid the regions of instability by changing the parameter values. This can, for instance, be done by lowering the gas velocity to increase the Damköhler number. If the bifurcations had occurred for another parameter, say γ, that could not be controlled, the situation would be different. Then there would be no way to avoid an unstable steady state of the system. Finally, another way to avoid unstable steady states of the system is to use a cooled reactor as it is shown to decrease the number of bifurcations and decrease the size of the areas of instability.

Chapter 10

Conclusion

The packed-bed reactor with an integrated heat exchanger was examined in this thesis. This included bifurcation analysis and simulations of the systems behaviour when subject to disturbances. At first the packed-bed reactor model without the heat exchanger was derived, discretized and implemented in MatLab. Simulations then showed that the packed-bed reactor works as an amplifier of disturbances because of the convective instability of the system. The system does however wash out any disturbances in time, meaning that all of the steady states were stable. Examination of the eigenvalues confirmed this and bifurcation analysis showed no bifurcations in a given parameter space, which covers many different processes in the chemical industry.

The heat exchanger was then modelled and integrated with the packed-bed reactor model. Simulations of the complete model showed that amplified disturbances are fed back to the reactor by the heat exchanger, where they are amplified again. This causes growing oscillations of temperature which in time turn into periodic oscillations. The system has this behaviour because Hopf bifurcations occur for some parameter values and give rise to these oscillations when the heat exchanger is integrated in the model. Furthermore, the occurrence of limit point bifurcations show that hysteresis can occur when certain parameters are varied. It is shown that the occurrence of bifurcations only depend on Da, β, α and $\Delta\lambda_{app}$ and as Da, β and α usually can be controlled by the operator of the reactor, most of the critical parameter values can be avoided altogether.
Finally it is concluded that there are fewer bifurcations and smaller areas of unstable steady

states when heat transfer to the reactor wall is assumed. This means that a cooled reactor would make the system more stable.

Chapter 11

Ideas for Future Work

It is clear that this report cannot cover all the aspects of bifurcation analysis of chemical reactors. Several topics in both mathematics and chemistry are used to cover this subject and some areas could be interesting to investigate further in another project.

For once, a different discretization scheme could be tried out. This could, for example, be the orthogonal collocation method as recommended in [5]. This method has two advantages. First, it would make it possible to analyse the effects of the Peclet numbers in the entire parameter space and second, the method needs fewer grid points, which would save time when doing simulations and bifurcation analysis with MatCont. This is although a very complicated method compared to the method of lines.

Some features can also be added to the model of the system. First of all, it takes some time for the gas to travel from the outlet of the heat exchanger to the inlet of the reactor and this time delay can be modelled in different ways. Second, in this report it was assumed that the heat exchanger has a constant temperature approach, ΔT_{app}. This is a simple model of the behaviour of a heat exchanger and using this model gives a good approximation of the ranges in which bifurcations can be found. The approach temperature normally varies though, depending on the temperatures of the inlet and outlet gas, so to get even more exact results one could try to implement this in the model.

Finally one can experiment with control equations to find out how to regulate α during the process to avoid regions of α that could cause instability.

Appendix A

MatLab Code

In this appendix all of the MatLab code used in the report can be found.

A.1 The Packed-Bed Reactor Model

The MatLab implementation of the packed-bed reactor model without heat transfer between the reaction mixture and the reactor wall is seen below.

```
1  function dy = SystemModel(~,y,par,Y10,Y20)
2  % This function implements a differential equation model for a packed-bed
3  % reactor without heat tranfer between the reaction mixture and the reactor
4  % wall.
5  % Input             y is a vector of function values.
6  %                   par is a vector containing the parameter values.
7  %                   Y10 is the inlet concentration.
8  %                   Y20 is the inlet temperature.
9  % Output            dy is a vector containing the derivatives of y.
10 % Programmer        Jan Langdeel Pedersen, 2013.
11
12 % ------------------------------------------------------------------------
13 % Initialization
14 % ------------------------------------------------------------------------
15 Le = par(1);
16 Da = par(2);
17 beta = par(3);
```

```
18 gamma = par(4);
19 Pem = par(5);
20 Peh = par(6);
21 N = par(7);
22 h = 1/(N+1);
23
24 y1 = y(1:N);
25 y2 = y(N+1:2*N);
26
27 % ------------------------------------------------------------------------
28 % y1
29 % ------------------------------------------------------------------------
30 A1 = diag(-Da*exp(gamma*(1-1./y2)),0);
31
32 B1 = (1/Pem)*(1/h^2)*(diag(-2*ones(N,1),0)+diag(ones(N-1,1),1)...
33     +diag(ones(N-1,1),-1));
34
35 C1 = -1/(2*h)*(diag(ones(N-1,1),1)+diag(-ones(N-1,1),-1));
36
37 % Robin BC at B1
38 y10 = (2*Pem*Y10*h-4*y1(1)+y1(2))/(2*Pem*h-3);
39
40 % Neumann BC at B2
41 y1N1 = 1/3*(4*y1(N)-y1(N-1));
42
43 % The approximated function values at the endpoints
44 G1 = zeros(N,1);
45 G1(1) = (1/Pem)*1/h^2*y10+1/(2*h)*y10;
46 G1(end) = (1/Pem)*1/h^2*y1N1-1/(2*h)*y1N1;
47
48 % The system of ODE's for y1
49 dy1 = (A1+B1+C1)*y1+G1;
50
51 % ------------------------------------------------------------------------
52 % y2
53 % ------------------------------------------------------------------------
54 A2 = -beta*A1;
55
```

```
56 B2 = Pem/Peh*B1;
57
58 C2 = C1;
59
60 % Robin BC at B1
61 y20 = (2*Peh*Y20*h-4*y2(1)+y2(2))/(2*Peh*h-3);
62
63 % Neumann BC at B2
64 y2N1 = 1/3*(4*y2(N)-y2(N-1));
65
66 % The approximated function values at the endpoints
67 G2 = zeros(N,1);
68 G2(1) = (1/Peh)*1/h^2*y20+1/(2*h)*y20;
69 G2(end) = (1/Peh)*1/h^2*y2N1-1/(2*h)*y2N1;
70
71 % The system of ODE's for y2
72 dy2 = 1/Le*(A2*y1+(B2+C2)*y2+G2);
73
74 % The complete system of ODE's
75 dy = [dy1;dy2];
```

A.2 Simulation of the Packed-Bed Reactor Model

The following script simulates the packed-bed reactor model without heat transfer between the reaction mixture and the reactor wall. In addition to this, the script also compares the steady states found to the steady states from [4].

```
% ------------------------------------------------------------------------
% Initialization
% ------------------------------------------------------------------------
Le = 3;
Da = 0.135;
beta = 0.5;
gamma = 22;
Pem = 3000;
Peh = 1000;

N = 200;
par = [Le; Da; beta; gamma; Pem; Peh; N];
tspan = [0 4];

b = 0.5; % Start of bed
L = 1; % length of bed

Y10 = 1;
Y20 = 1;

% The initial conditions
y0 = zeros(2*N,1);
y0(1:N) = 0;
y0(N+1:2*N) = 1;

% ------------------------------------------------------------------------
% Simulation
% ------------------------------------------------------------------------
[t,y] = ode15s(@SystemModel,tspan,y0,[],par,Y10,Y20);
y1 = y(:,1:N);
y2 = y(:,N+1:2*N);
```

```
32
33 % ------------------------------------------------------------------------
34 % Plotting
35 % ------------------------------------------------------------------------
36 y1 = y1(:,N/2+1:N);
37 y2 = y2(:,N/2+1:N);
38 l = linspace(b,L,N/2);
39
40 % Simulation of the concentration
41 hold on
42 plot(l,y1(round(length(t)*1/4),:),'b-','LineWidth',2)
43 plot(l,y1(round(length(t)*2/4),:),'g-','LineWidth',2)
44 plot(l,y1(round(length(t)*3/4),:),'r-','LineWidth',2)
45 plot(l,y1(end,:),'c-','LineWidth',2);
46 hold off
47
48 xlabel('Dimensionless length, x')
49 ylabel('Dimensionless concentration, y1')
50 legend('\tau = 1','\tau = 2','\tau = 3','\tau = 4','Location','SouthWest')
51 fh = figure(1);
52 set(fh,'color','white')
53 set(gca,'box','off')
54
55 % Simulation of the temperature
56 figure
57 hold on
58 plot(l,y2(round(length(t)*1/4),:),'b-','LineWidth',2)
59 plot(l,y2(round(length(t)*2/4),:),'g-','LineWidth',2)
60 plot(l,y2(round(length(t)*3/4),:),'r-','LineWidth',2)
61 plot(l,y2(end,:),'c-','LineWidth',2);
62 hold off
63
64 xlabel('Dimensionless length, x')
65 ylabel('Dimensionless temperature, y2')
66 legend('\tau = 1','\tau = 2','\tau = 3','\tau = 4','Location','NorthWest')
67 fh = figure(2);
68 set(fh,'color','white')
69 set(gca,'box','off')
```

```
70
71 % Three-dimensional plots
72 h = 1/(N+1);
73 z = (h:h:N*h)';
74 yp1 = y(:,1:N);
75 yp2 = y(:,N+1:2*N);
76
77 figure
78 mesh(z,t,yp1)
79 title('Dimensionless concentration'); xlabel('Dimensionless length, x');
80 ylabel('Dimensionless Time, \tau');
81 fh = figure(3); set(fh,'color','white'); set(gca,'box','off');
82
83 figure
84 mesh(z,t,yp2)
85 title('Dimensionless temperature'); xlabel('Dimensionless length, x');
86 ylabel('Dimensionless time,\tau');
87 fh = figure(4); set(fh,'color','white'); set(gca,'box','off')
88
89 % ------------------------------------------------------------------------
90 % Reconstruction of the steady state plot from the article 'Convective
91 % instability and its suppression in packed-bed- and monolith reactors'
92 % ------------------------------------------------------------------------
93 % Concentration
94 art1 = load('SteadyStateConcentration.txt');
95 x1art = art1(:,1);
96 y1art = art1(:,2);
97
98 yi1 = interp1(x1art,y1art,l); % Interpolation
99
100 figure
101 hold on
102 plot(l,y1(end,:),'b-','LineWidth',2);
103 plot(l,yi1,'.r');
104 hold off
105
106 axis([0.5 1 0 0.9])
107 xlabel('Dimensionless length, x')
```

```
108 ylabel('Dimensionless concentration, y1')
109 legend('Simulation of Steady State','Steady State Simulation from [4]',...
110     'Location','SouthWest')
111 fh = figure(5);
112 set(fh,'color','white')
113 set(gca,'box','off')
114
115 figure
116 plot(l,y1(end,:)-yi1,'g-','LineWidth',2);
117 xlabel('Dimensionless length, x')
118 ylabel('Residual')
119 fh = figure(6);
120 set(fh,'color','white')
121 set(gca,'box','off')
122
123 % Temperature
124 art2 = load('SteadyStateTemperature.txt');
125 x2art = art2(:,1);
126 y2art = art2(:,2);
127
128 yi2 = interp1(x2art,y2art,l); % Interpolation
129
130 figure
131 hold on
132 plot(l,y2(end,:),'b-','LineWidth',2);
133 plot(l,yi2,'.r');
134 hold off
135
136 xlabel('Dimensionless length, x')
137 ylabel('Dimensionless temperature, y2')
138 legend('Simulation of Steady State','Steady State Simulaion from [4]',...
139     'Location','SouthEast')
140 fh = figure(7);
141 set(fh,'color','white')
142 set(gca,'box','off')
143
144 figure
145 plot(l,y2(end,:)-yi2,'g-','LineWidth',2);
```

```
146 xlabel('Dimensionless length, x')
147 ylabel('Residual')
148 fh = figure(8);
149 set(fh,'color','white')
150 set(gca,'box','off')
```

A.3 The Packed-Bed Reactor Model with Heat Transfer to the Reactor Wall

The MatLab implementation of the packed-bed reactor model with heat transfer between the reaction mixture and the reactor wall is see below.

```
1  function dy = SystemModelWall(~,y,par,Y10,Y20)
2  % This function implements a differential equation model for a packed-bed
3  % reactor with heat tranfer between the reaction mixture and the reactor
4  % wall.
5  % Input             y is a vector of function values.
6  %                   par is a vector containing the parameter values.
7  %                   Y10 is the inlet concentration.
8  %                   Y20 is the inlet temperature.
9  % Output            dy is a vector containing the derivatives of y.
10 % Programmer        Jan Langdeel Pedersen, 2013.
11
12 % ------------------------------------------------------------------------
13 % Initialization
14 % ------------------------------------------------------------------------
15 Le = par(1);
16 Da = par(2);
17 beta = par(3);
18 gamma = par(4);
19 Pem = par(5);
20 Peh = par(6);
21 Hw = par(7);
22 y2w = par(8);
23 N = par(9);
24 h = 1/(N+1);
25
26 y1 = y(1:N);
27 y2 = y(N+1:2*N);
28
29 % ------------------------------------------------------------------------
30 % y1
31 % ------------------------------------------------------------------------
```

```
32 A1 = diag(-Da*exp(gamma*(1-1./y2)),0);
33
34 B1 = (1/Pem)*(1/h^2)*(diag(-2*ones(N,1),0)+diag(ones(N-1,1),1)...
35     +diag(ones(N-1,1),-1));
36
37 C1 = -1/(2*h)*(diag(ones(N-1,1),1)+diag(-ones(N-1,1),-1));
38
39 % Robin BC at B1
40 y10 = (2*Pem*Y10*h-4*y1(1)+y1(2))/(2*Pem*h-3);
41
42 % Neumann BC at B2
43 y1N1 = 1/3*(4*y1(N)-y1(N-1));
44
45 % The approximated function values at the endpoints
46 G1 = zeros(N,1);
47 G1(1) = (1/Pem)*1/h^2*y10+1/(2*h)*y10;
48 G1(end) = (1/Pem)*1/h^2*y1N1-1/(2*h)*y1N1;
49
50 % The system of ODE's for y1
51 dy1 = (A1+B1+C1)*y1+G1;
52
53 % ------------------------------------------------------------------------
54 % y2
55 % ------------------------------------------------------------------------
56 A2 = -beta*A1;
57
58 B2 = Pem/Peh*B1;
59
60 C2 = C1;
61
62 H2 = -diag(Hw*ones(N,1),0);
63
64 W2 = Hw*y2w*ones(N,1);
65
66 % Robin BC at B1
67 y20 = (2*Peh*Y20*h-4*y2(1)+y2(2))/(2*Peh*h-3);
68
69 % Neumann BC at B2
```

```
70 y2N1 = 1/3*(4*y2(N)-y2(N-1));
71
72 % The approximated function values at the endpoints
73 G2 = zeros(N,1);
74 G2(1) = (1/Peh)*1/h^2*y20+1/(2*h)*y20;
75 G2(end) = (1/Peh)*1/h^2*y2N1-1/(2*h)*y2N1;
76
77 % The system of ODE's for y2
78 dy2 = 1/Le*(A2*y1+(B2+C2+H2)*y2+G2+W2);
79
80 % The complete system of ODE's
81 dy = [dy1;dy2];
```

A.4 Simulations with Disturbances

The following script simulates the packed-bed reactor model subject to a disturbance to the inlet conditions.

```
% ------------------------------------------------------------------------
% Initialization
% ------------------------------------------------------------------------
Le = 3;
Da = 0.135;
beta = 0.5;
gamma = 22;
Pem = 3000;
Peh = 1000;
N = 400;
par = [Le; Da; beta; gamma; Pem; Peh; N];

% ------------------------------------------------------------------------
% Simulation
% ------------------------------------------------------------------------
% The initial condition
y0 = zeros(2*N,1);
y0(1:N) = 0;
y0(N+1:2*N) = 1;
[~,y] = ode15s(@SystemModel,[0 400],y0,[],par,1,1);
y1 = y(:,1:N);
y2 = y(:,N+1:end);
y10s = y1(end,:)';
y20s = y2(end,:)';

% Time loop
NTime    = 100; % Number of simulations
t_sim    = 10; % End time
t_span   = linspace(0,t_sim,NTime);
Y1 = []; Y2 = []; T = [];

y1_0 = ones(size(t_span));
```

```
y2_0 = y1_0;
y0 = [y10s;y20s];

for n = 1:NTime-1
    if n > NTime/5
        y2_0(n) = 0.95; %Step change in temperature
    end

    [t,y] = ode15s(@SystemModel,[t_span(n) t_span(n+1)],y0...
        ,[],par,y1_0(n),y2_0(n));
    y1 = y(:,1:N);
    y2 = y(:,N+1:end);

    %New initial state
    y0(1:N)     = y1(end,:);
    y0(N+1:end) = y2(end,:);

    %Storage of solution
    Y1 = [Y1; y1]; Y2 = [Y2; y2]; T = [T; t];
end

% ------------------------------------------------------------------------
% Plotting
% ------------------------------------------------------------------------
h = 1/(N+1);
z = (h:h:N*h)';

figure
mesh(z,T,Y1)
title('Dimensionless Concentration'); xlabel('Dimensionless Length, x');
ylabel('Dimensionless Time, \tau');
fh = figure(1); set(fh,'color','white'); set(gca,'box','off');

figure
mesh(z,T,Y2)
title('Dimensionless Temperature'); xlabel('Dimensionless Length, x');
ylabel('Dimensionless Time, \tau');
fh = figure(2); set(fh,'color','white'); set(gca,'box','off')
```

```
71
72 figure
73 hold on
74 plot(z,Y1(1,:),'b-','LineWidth',2)
75 plot(z,Y1(round(length(T)*0.3),:),'r-','LineWidth',2)
76 plot(z,Y1(round(length(T)*0.6),:),'g-','LineWidth',2)
77 plot(z,Y1(end,:),'c-','LineWidth',2)
78 title('Dimensionless Concentration profiles');
79 xlabel('Dimensionless Length, x'); ylabel('Dimensionless Concentration, y_1');
80 legend('t = 0', 't = 3', 't = 6', 't = 10');
81 fh = figure(3); set(fh,'color','white'); set(gca,'box','off')
82 hold off
83
84 figure
85 hold on
86 plot(z,Y2(1,:),'b-','LineWidth',2)
87 plot(z,Y2(round(length(T)*0.3),:),'r-','LineWidth',2)
88 plot(z,Y2(round(length(T)*0.6),:),'g-','LineWidth',2)
89 plot(z,Y2(end,:),'c-','LineWidth',2)
90 title('Dimensionless Temperature profiles');
91 xlabel('Dimensionless Length, x'); ylabel('Dimensionless Temperature, y_2');
92 legend('t = 0', 't = 3', 't = 6', 't = 10');
93 fh = figure(4); set(fh,'color','white'); set(gca,'box','off')
94 hold off
```

A.5 The MatCont System File

The MatCont system file is seen below. The initial condition is found by simulating the steady state with the initial parameter values with twice as many grid points as specified by the user. By using this simulation an initial condition, a new steady state simulation is then performed with the user-specified number of grid points. In this way, an accurate steady state is calculated and the continuation can be performed with fewer grid points.

```
function out = PackedBedSystem
out{1} = @init;
out{2} = @fun_eval;
out{3} = [];
out{4} = [];
out{5} = [];
out{6} = [];
out{7} = [];
out{8} = [];
out{9} = [];

% ------------------------------------------------------------------------
function dfdt = fun_eval(~,y,N,Da,Le,beta,gamma,Pem,Peh)
y1 = y(1:N);
y2 = y(N+1:2*N);
h = 1/(N+1);

% ------------------------------------------------------------------------
% y1
% ------------------------------------------------------------------------
A1 = diag(-Da*exp(gamma*(1-1./y2)),0);

B1 = (1/Pem)*(1/h^2)*(diag(-2*ones(N,1),0)+diag(ones(N-1,1),1)...
    +diag(ones(N-1,1),-1));

C1 = -1/(2*h)*(diag(ones(N-1,1),1)+diag(-ones(N-1,1),-1));

% Robin BC at B1
y10 = (2*Pem*h-4*y1(1)+y1(2))/(2*Pem*h-3);
```

```
30
31 % Neumann BC at B2
32 y1N1 = 1/3*(4*y1(N)-y1(N-1));
33
34 % The approximated function values at the endpoints
35 G1 = zeros(N,1);
36 G1(1) = (1/Pem)*1/h^2*y10+1/(2*h)*y10;
37 G1(end) = (1/Pem)*1/h^2*y1N1-1/(2*h)*y1N1;
38
39 % The system of ODE's for y1
40 dy1 = (A1+B1+C1)*y1+G1;
41
42 % ------------------------------------------------------------------------
43 % y2
44 % ------------------------------------------------------------------------
45 A2 = -beta*A1;
46
47 B2 = Pem/Peh*B1;
48
49 C2 = C1;
50
51 % Robin BC at B1
52 y20 = (2*Pem*h-4*y2(1)+y2(2))/(2*Pem*h-3);
53
54 % Neumann BC at B2
55 y2N1 = 1/3*(4*y2(N)-y2(N-1));
56
57 % The approximated function values at the endpoints
58 G2 = zeros(N,1);
59 G2(1) = (1/Peh)*1/h^2*y20+1/(2*h)*y20;
60 G2(end) = (1/Peh)*1/h^2*y2N1-1/(2*h)*y2N1;
61
62 % The system of ODE's for y2
63 dy2 = 1/Le*(A2*y1+(B2+C2)*y2+G2);
64
65 % The complete system of ODE's
66 dfdt = [dy1;dy2];
67 dfdt = sparse(dfdt);
```

```
68
69 % ------------------------------------------------------------------------
70 function [tspan,y0,options] = init(N,Da,Le,beta,gamma,Pem,Peh)
71 N2 = 2*N;
72 par = [Le; Da; beta; gamma; Pem; Peh; N2];
73 tspan1 = 0;
74 tspan2 = 150;
75 tspan = [tspan1 tspan2];
76
77 % The initial conditions
78 y0 = zeros(2*N2,1);
79 y0(1:N2) = 0;
80 y0(N2+1:2*N2) = 1;
81
82 [~,yss] = ode15s(@SystemModel,tspan,y0,[],par);
83 y1ss = yss(:,1:N2);
84 y2ss = yss(:,N2+1:2*N2);
85 y10ss = y1ss(end,:);
86 y20ss = y2ss(end,:);
87
88 % Removing half the points
89 Y1ss = zeros(N,1);
90 Y2ss = Y1ss;
91 for i = 1:N
92     Y1ss(i) = y10ss(2*i);
93     Y2ss(i) = y20ss(2*i);
94 end
95
96 y0ss = [Y1ss; Y2ss];
97
98 % Simulation with half the number of mesh points
99 par = [Le; Da; beta; gamma; Pem; Peh; N];
100 tspan = [tspan2 tspan2+1];
101 [~,y2] = ode15s(@SystemModel,tspan,y0ss,[],par);
102
103 y12 = y2(:,1:N);
104 y22 = y2(:,N+1:2*N);
105 y01 = y12(1,:);
```

```
106 y02 = y22(1,:);
107 y0 = [y01, y02]';
108
109 handles = feval(@PackedBedSystem);
110 options = odeset('Vectorized','on');
```

A.6 The MatCont Script File

The MatLab script that actually creates the bifurcation diagrams is seen below.

```
% Initialization
global cds
N = 82; Da = 1; Le = 40; beta = 0.25; gamma = 11; Pem = 1000; Peh = 1000;
ap = 2; % The active parameter
par = [N;Da;Le;beta;gamma;Pem;Peh];
handles = feval(@PackedBedSystem);
[~,y0,options] = feval(handles{1},N,Da,Le,beta,gamma,Pem,Peh);

% Initial information is computed
[y1,v1] = init_EP_EP(@PackedBedSystem,y0,par,ap);

% Options
MaxNumPoints = 550;
opt = contset;
opt = contset(opt,'MaxNumPoints',MaxNumPoints);
opt = contset(opt,'Backward',1);
opt = contset(opt,'Eigenvalues',1);

% The continuation
[y,v,s,h,f] = cont(@pde_1,y1,v1,opt);

% Diagrams at the end point
cpl(y,v,s,[2*N+1 N]); xlabel('Da'); ylabel('y_1(N)');
fh = figure(1);
set(fh,'color','white')

figure
cpl(y,v,s,[2*N+1 2*N]); xlabel('Da'); ylabel('y_2(N)');
fh = figure(2); set(fh,'color','white')

figure
cpl(y,v,s,[2*N+1 3]); xlabel('Da'); ylabel('y_1(1)');
fh = figure(3); set(fh,'color','white')

```

```
35 figure
36 cpl(y,v,s,[2*N+1 N+3]); xlabel('Da'); ylabel('y_2(1)');
37 fh = figure(4); set(fh,'color','white')
```

A.7 The Complete System Model

The MatLab implementation of the complete model is seen below.

```
1  function dy = SystemModelFBWall(~,y,par,Y10,Y20)
2  % This function implements a differential equation model for a packed-bed
3  % reactor with heat tranfer between the reaction mixture and the reactor
4  % wall and an integrated heat exchanger.
5  % Input             y is a vector of function values.
6  %                   par is a vector containing the parameter values.
7  %                   Y10 is the inlet concentration.
8  %                   Y20 is the inlet temperature.
9  % Output            dy is a vector containing the derivatives of y.
10 % Programmer        Jan Langdeel Pedersen, 2013.
11
12 % ------------------------------------------------------------------------
13 % Initialization
14 % ------------------------------------------------------------------------
15 Le = par(1);
16 Da = par(2);
17 beta = par(3);
18 gamma = par(4);
19 Pem = par(5);
20 Peh = par(6);
21 Hw = par(7);
22 y2w = par(8);
23 dTapp = par(9);
24 alpha = par(10);
25 N = par(11);
26 h = 1/(N+1);
27
28 y1 = y(1:N);
29 y2 = y(N+1:2*N);
30 T3 = y2(end);
31
32 T1 = T3-dTapp;
33 T2 = alpha*Y20+(1-alpha)*T1;
34 lambda2 = T2;
```

```
35
36 % ------------------------------------------------------------------------
37 % y1
38 % ------------------------------------------------------------------------
39 A1 = diag(-Da*exp(gamma*(1-1./y2)),0);
40
41 B1 = (1/Pem)*(1/h^2)*(diag(-2*ones(N,1),0)+diag(ones(N-1,1),1)...
42     +diag(ones(N-1,1),-1));
43
44 C1 = -1/(2*h)*(diag(ones(N-1,1),1)+diag(-ones(N-1,1),-1));
45
46 % Robin BC at B1
47 y10 = (2*Pem*Y10*h-4*y1(1)+y1(2))/(2*Pem*h-3);
48
49 % Neumann BC at B2
50 y1N1 = 1/3*(4*y1(N)-y1(N-1));
51
52 % The approximated function values at the endpoints
53 G1 = zeros(N,1);
54 G1(1) = (1/Pem)*1/h^2*y10+1/(2*h)*y10;
55 G1(end) = (1/Pem)*1/h^2*y1N1-1/(2*h)*y1N1;
56
57 % The system of ODE's for y1
58 dy1 = (A1+B1+C1)*y1+G1;
59
60 % ------------------------------------------------------------------------
61 % y2
62 % ------------------------------------------------------------------------
63 A2 = -beta*A1;
64
65 B2 = Pem/Peh*B1;
66
67 C2 = C1;
68
69 H2 = -diag(Hw*ones(N,1),0);
70
71 W2 = Hw*y2w*ones(N,1);
72
```

```
73 % Robin BC at B1
74 y20 = (2*Peh*lambda2*h-4*y2(1)+y2(2))/(2*Peh*h-3);
75
76 % Neumann BC at B2
77 y2N1 = 1/3*(4*y2(N)-y2(N-1));
78
79 % The approximated function values at the endpoints
80 G2 = zeros(N,1);
81 G2(1) = (1/Peh)*1/h^2*y20+1/(2*h)*y20;
82 G2(end) = (1/Peh)*1/h^2*y2N1-1/(2*h)*y2N1;
83
84 % The system of ODE's for y2
85 dy2 = 1/Le*(A2*y1+(B2+C2+H2)*y2+G2+W2);
86
87 % The complete system of ODE's
88 dy = [dy1;dy2];
```

Bibliography

[1] H. Scott Fogler

Elements of Chemical Reaction Engineering, 3rd Ed

Prentice-Hall, 1999

[2] *Tekniknoter til Kursus 36260 - Matematisk Analyse og Modeller for Kemiske Systemer*

Institut for Kemiteknik, Danmarks Tekniske Universitet, August 2000

[3] Randall J. LeVeque

Finite Difference Methods for Ordinary and Partial Differential Equations

SIAM, 2007

[4] V. Z. Yakhnin, M. Menzinger

Convective Instability and its Suppression in Packed-bed- and Monolith Reactors

Chemical Engineering Science 54, 1999, page 4547-4557

[5] Klavs F. Jensen, W. Harmon Ray

The Bifurcation Behavior of Tubular Reactors

Chemical Engineering Science Vol. 37, No. 2, pp. 199-222, 1982

[6] A.B. Rovinsky, M. Menzinger

Self-organization induced by a differential flow

Physical Review Letters, 70, 778-781, 1993

[7] V. Z. Yakhnin, A. B. Rovinsky, M. Menzinger

Convective Instability Induced by Differential Transport in the Tubular Packed-Bed Reactor

Chemical Engineering Science Vol. 50, No. 18, pp. 2853-2859, 1995

[8] V. Z. Yakhnin, M. Menzinger
Moving Hot Spots and Resonance in Adiabatic Packed-Bed Reactors
The American Institute of Chemical Engineers Journal, 44, 1222-1225, 1998

[9] Vemuri Balakotaiah, Sandra M. S. Dommeti, Nikunj Gupta
Bifurcation Analysis of Chemical Reactors and Reacting Flows
Chaos, Volume 9, Number 1, 1999

[10] P. V. Danckwerts
Continuous Flow Systems. Distribution of Residence Times
Chemical Engineering Science Vol. 2, Issue 1, pp. 1-13, 1953

[11] *www.digitizer.sourceforge.net*

[12] *www.sourceforge.net/projects/matcont*

[13] Kenneth B. Bischoff
A Note on Boundary Conditions for Flow Reactors
Chemical Engineering Science Vol. 16, Nos 1 and 2. December 1961

[14] Peter Atkins, Julio De Paula
Physical Chemistry, Ninth Edition
W. H. Freeman and Company, 2010

[15] *www.sourceforge.net/projects/matcont/files/Documentation*

[16] Steven H. Strogatz
Nonlinear Dynamics and Chaos
Westview Press, 2000

[17] Ole Christensen
Differentialligninger og Uendelige Rækker
Institut for Matematik, Danmarks Tekniske Universitet, 2009